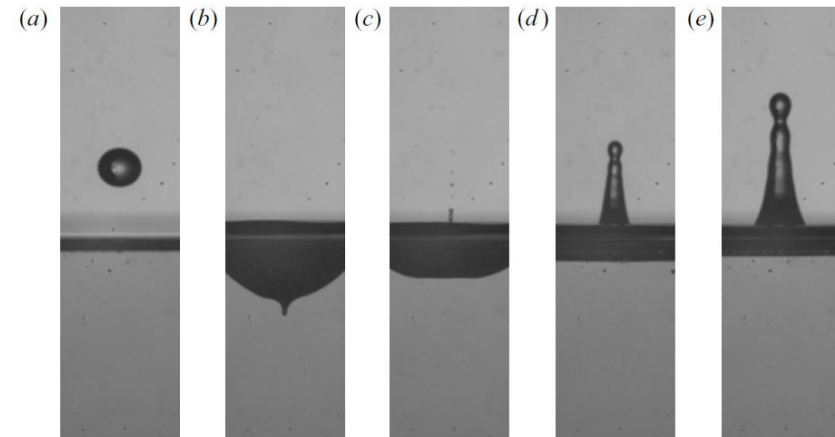


From drop splashing to Worthington jets

José Manuel Gordillo, Universidad de Sevilla, SPAIN

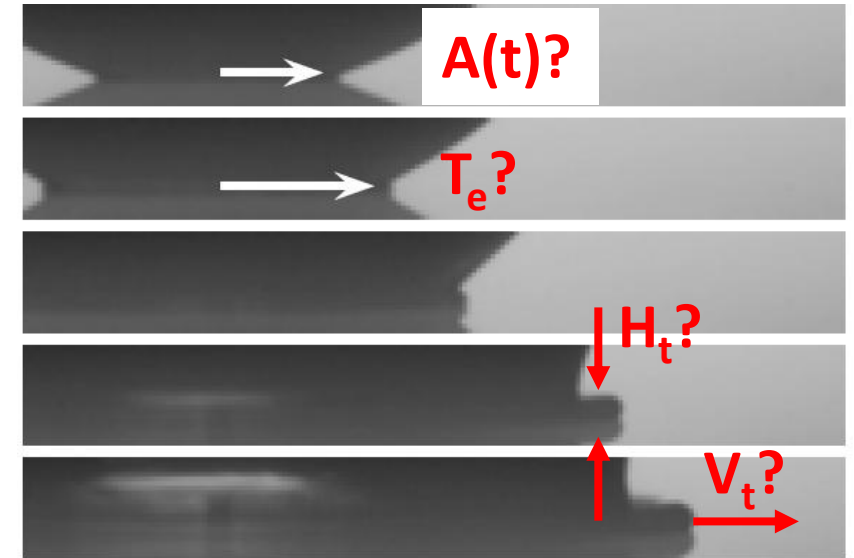
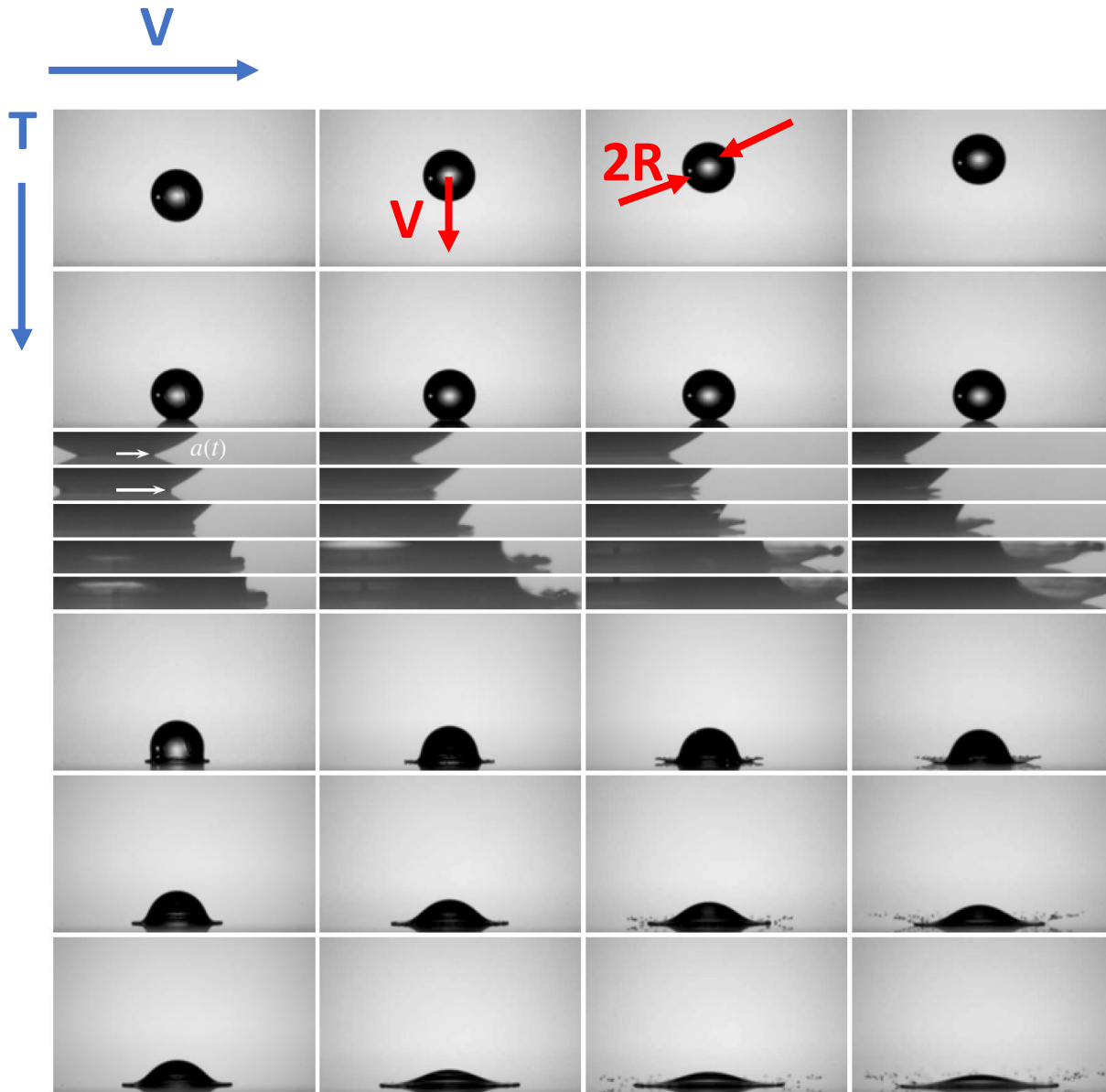


This work has been supported by the Grant PID
PID2020-115655G, financed by the Spanish MCIN/AEI/
10.13039/501100011033



Universidad de Sevilla

SPLASH TRANSITION FOR A DROP IMPACTING A DRY SUBSTRATE: POTENTIAL FLOW THEORY



Questions to solve using potential flow theory

Wetted radius $A(t)?$

Ejection time $T_e?$

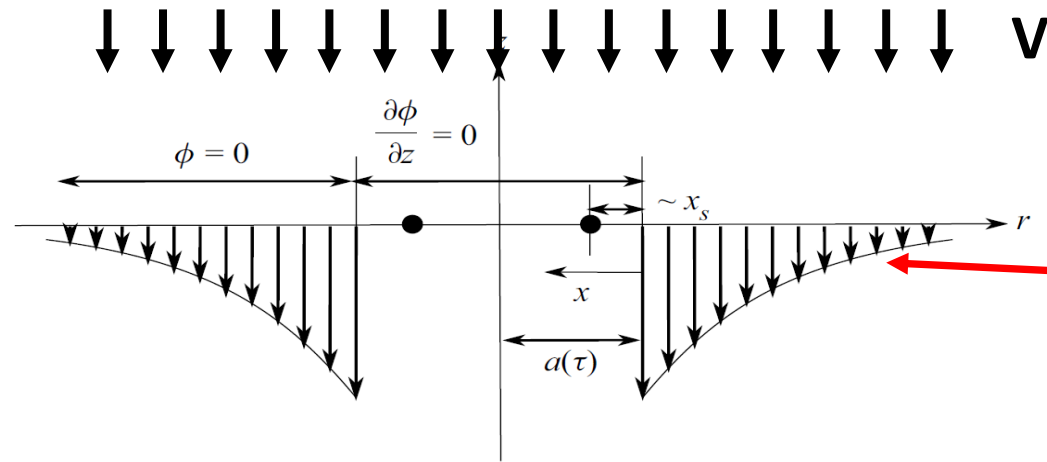
Thickness of the lamella $H_t(t)?$

Velocity of the lamella $V_t(t)?$

R , V , R/V and ρV^2 as characteristic scales

WETTED RADIUS A(T) CALCULATED USING THE WAGNER CONDITION

Which is nothing but the interfacial kinematic boundary condition integrated in time using the analytical velocity field obtained solving the Laplace equation subjected to the far field boundary condition, which expresses that the velocity is uniform and equal to V, to the impenetrability B.C. and to the B.C. for the velocity potential ϕ at the free interface deduced by means of the Bernoulli equation in the limit $t \ll 1$ namely, neglecting the contribution of the kinetic energy per unit volume. This equation provides the time at which a point in a fixed radial position of a parabola i.e. the shape of the drop near the minimum, reaches the wall.



The solution of the Laplace equation, provides with the Following expression for the velocity at the free interface

$$\mathbf{k} \cdot \mathbf{u} = -1 - \frac{2}{\pi} \left[\frac{a}{\sqrt{r^2 - a^2}} - \arcsin \left(\frac{a}{r} \right) \right]$$

$$\frac{R}{2} \left(\frac{A}{R} \right)^2 - VT - \frac{2V}{\pi} \left[\int_0^T \frac{\kappa(\tau) d\tau}{\sqrt{A(T)^2 - \kappa(\tau)^2}} - \int_0^T \arcsin \left(\frac{\kappa(\tau)}{A(T)} \right) d\tau \right] = 0,$$

$$\Rightarrow a^2 - 2t - \frac{4}{\pi} \int_0^a \left[\frac{\kappa}{\sqrt{a^2 - \kappa^2}} - \arcsin \left(\frac{\kappa}{a} \right) \right] \frac{d\tau}{d\kappa} d\kappa = 0,$$

$$a = \sqrt{3t}.$$

However, the solution for the velocity field at the free interface is not uniformly valid because it diverges for $r \approx a$ where $u \approx -(1/\pi)\sqrt{2a/x}$, with $r=a+x$ and $x \ll 1$. Hence, in a region close to the wetted radius, the term $\rho|\nabla\phi|^2/2$ needs to be retained in the Euler-Bernoulli equation.

Expresses that, since the flow is quasi steady in the region of length H_t , the modulus of the velocity in the frame of reference moving with the velocity da/dt is conserved along the free surface, which is a streamline, and that the maximum pressure, which is the stagnation pressure, is attained at a distance $\sim H_t$ from the root of the lamella



In the laboratory frame of reference the liquid velocity within the lamella is

Finally, the thickness of the lamella is deduced by mass conservation, imposing that the flow rate through the lamella, in the inner region, is the one is posed by the outer solution at the root of the lamella:

week ending
11 JULY 2014



OUR DESCRIPTION RATIONALIZES THE EXPERIMENTS REPORTED ON THE SPLASH TRANSITION FOR ARBITRARY VALUES OF THE ATMOSPHERIC PRESSURE AND ALSO PERMITS TO PREDICT THE DIAMETERS AND VELOCITIES OF THE DROPS EJECTED WHEN $V > V^*$

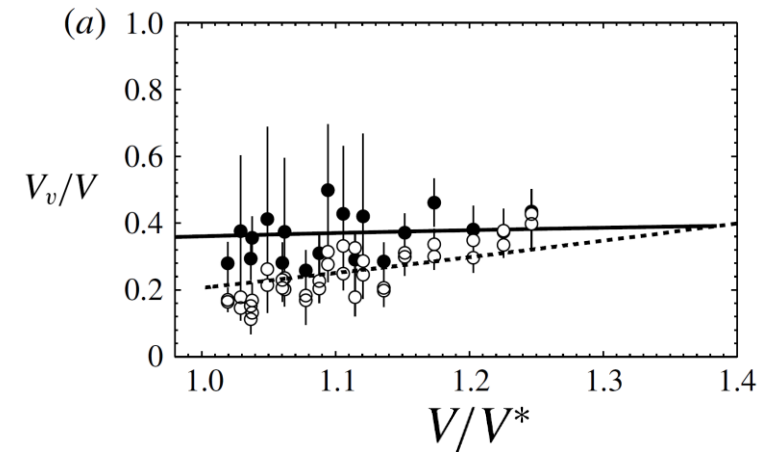
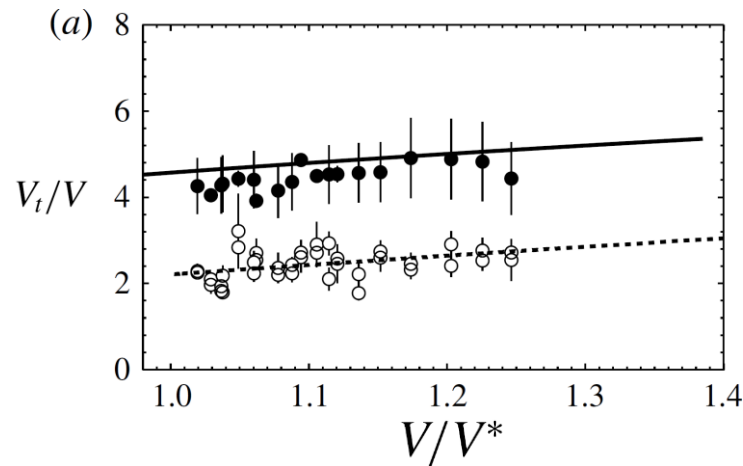
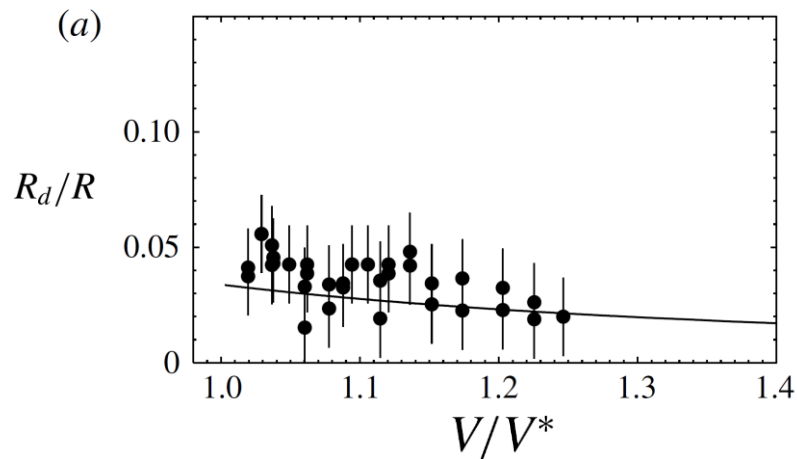


J. Fluid Mech. (2015), vol. 772, pp. 630–648. © Cambridge University Press 2015
doi:10.1017/jfm.2015.223

630

The diameters and velocities of the droplets ejected after splashing

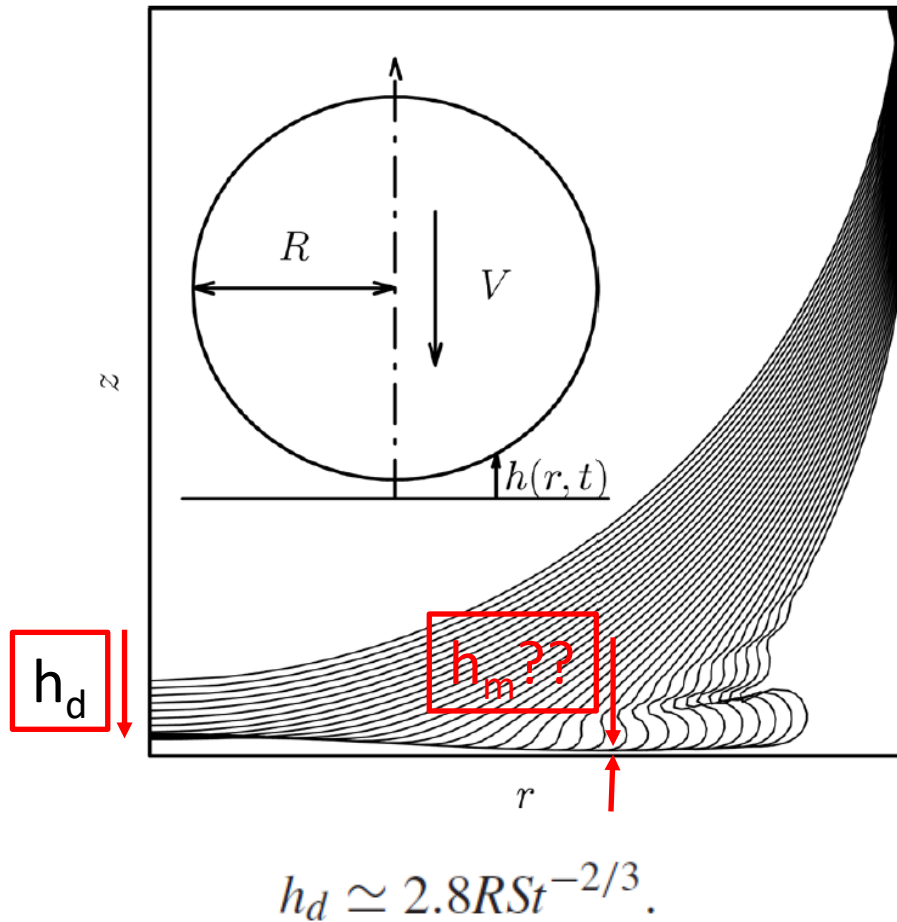
Guillaume Riboux¹ and José Manuel Gordillo^{1,†}



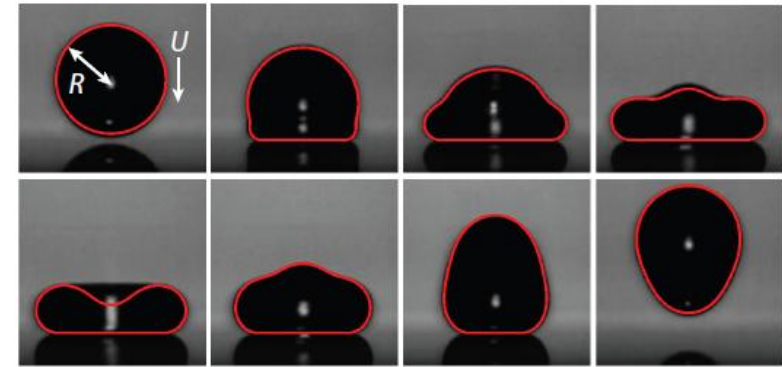
Annual Review of Fluid Mechanics

Gas Microfilms in Droplet Dynamics: When Do Drops Bounce?

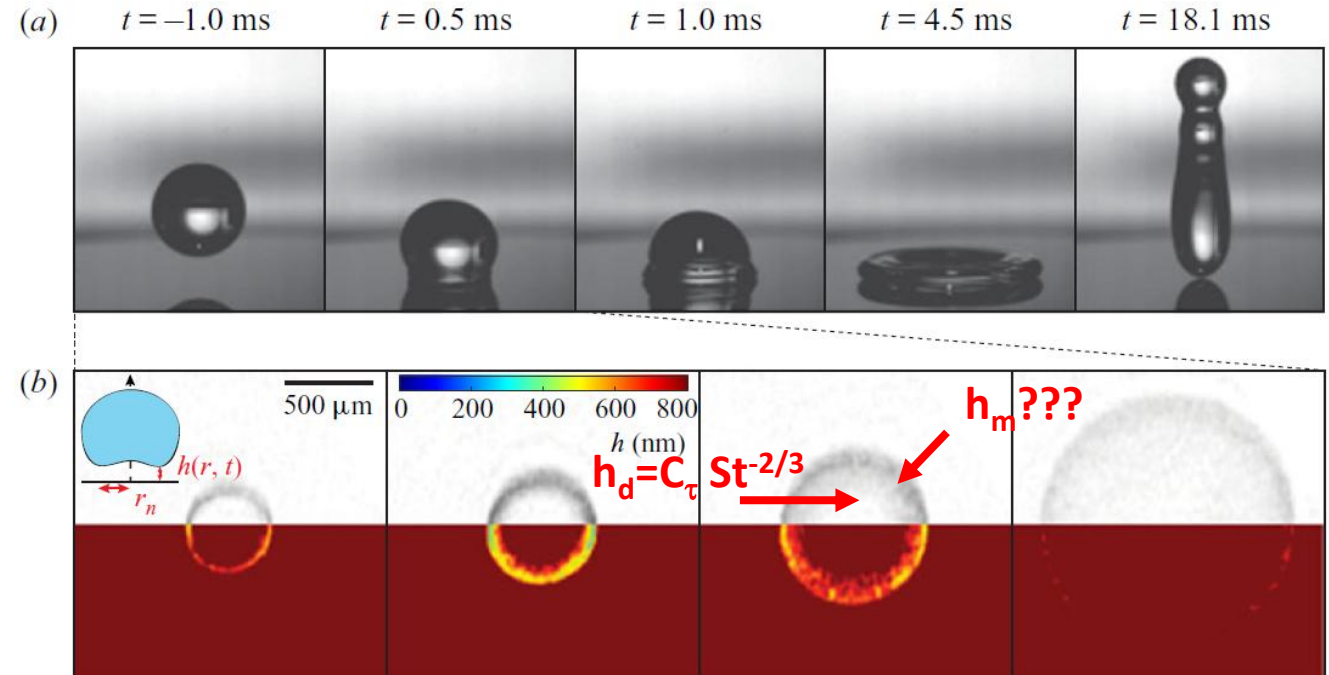
James E. Sprittles



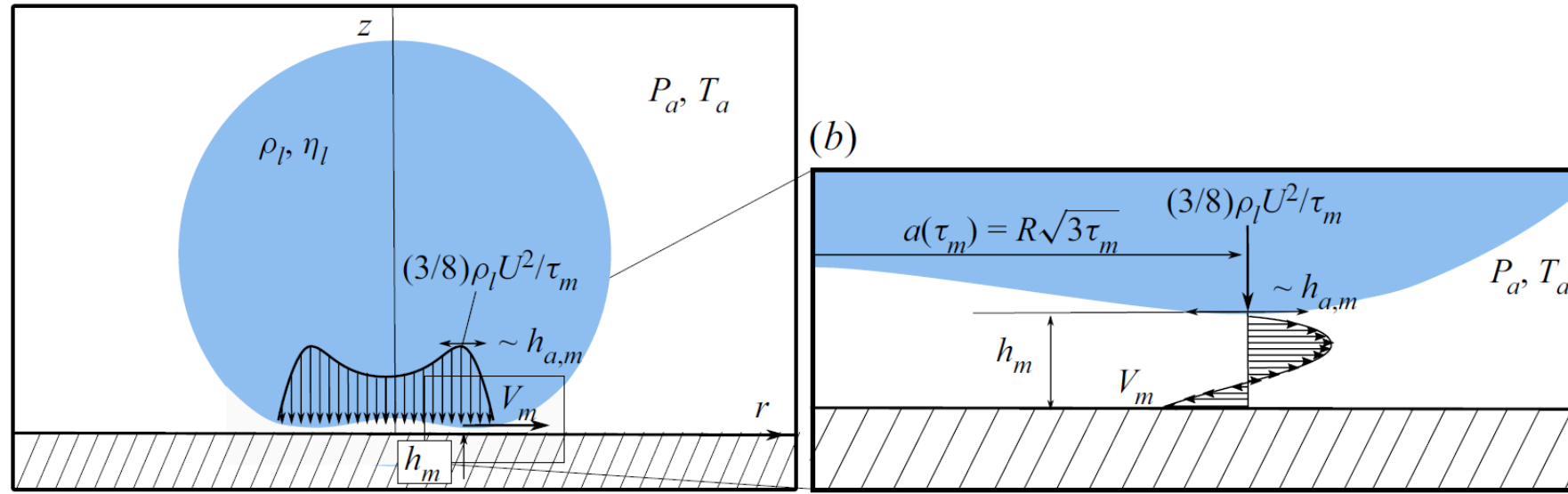
De Ruiter et al, Nat. Phys. 2015



Chantelot and Lohse, JFM 2021



OUR THEORY FOR THE SCALING OF h_m DIFFERS FROM THE CLASSICAL RESULTS OF MANDRE AND BRENNER, PRL 2009 AND JFM 2012

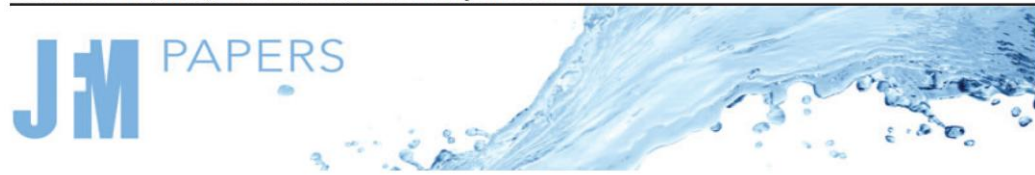


OUR MECHANISM: The liquid does not touch the wall thanks to the classical lubrication mechanism in the slightly convergent geometry formed between the liquid and the wall near the minimum: the Couette flow in the moving frame of reference balances the Poiseuille flow induced by the pressure gradient calculated at the region where the pressure is maximum:

WE OBTAIN h_m FROM THE MASS BALANCE:

$$\frac{V_m h_m}{2} \simeq \frac{1}{h_{a,m}} \frac{h_m^3}{12\eta_a} \frac{\rho_l V_m^2}{2}$$

WE NEED TO KNOW THE VALUE OF THE PRESSURE GRADIENT (POISEUILLE FLOW) AT THE MINIMUM HEIGHT AS WELL AS THE TANGENTIAL VELOCITY (COUETTE FLOW) AT THIS LOCATION AS WELL.



Liquid pressure and velocity at the periphery of the entrapped bubble using potential flow theory

The initial impact of drops cushioned by an air or vapour layer with applications to the dynamic Leidenfrost regime

José M. Gordillo^{1,†} and Guillaume Riboux¹

PRL 113, 024507 (2014)

PHYSICAL REVIEW LETTERS

Experiments of Drops Impacting a Smooth Solid Surface: A Model of the Critical Impact Speed for Drop Splashing

Guillaume Riboux and José Manuel Gordillo*

Potential flow expressions particularized at the instant $t = C_\tau St^{-2/3}$ at which the central bubble is entrapped
 $St = \rho VR / \mu_a$

Maximum liquid pressure is attained at a distance from the axis of symmetry: $a_m = \sqrt{3C_\tau} St^{-1/3}$

$V_m = V(\tau_m) = U \frac{\sqrt{3}}{2} C_\tau^{-1/2} St^{1/3}$, ← Tangential liquid velocity where the maximum pressure is attained

$\Delta p_m = \Delta p(\tau_m) = \frac{3}{8C_\tau} \rho_l U^2 St^{2/3}$, ← Maximum pressure with $C_\tau \simeq 12.4$,

$h_{a,m} = h_a(\tau_m) = R \frac{\sqrt{12C_\tau^3}}{3\pi} St^{-1}$. ← Length along which pressure changes of the order of Δp_m take place when capillary effects are negligible

When capillary effects cannot be neglected, pressure changes take place in a length given by

$$\frac{\gamma h_m}{\ell_c^2} \sim \Delta p_m \Rightarrow \ell_c \sim \sqrt{\frac{\gamma h_m}{\Delta p_m}} = \sqrt{\frac{8C_\tau}{3}} \sqrt{Rh_m} We^{-1/2} St^{-1/3}$$

with $C_\tau \simeq 12.4$,

Inertial regime

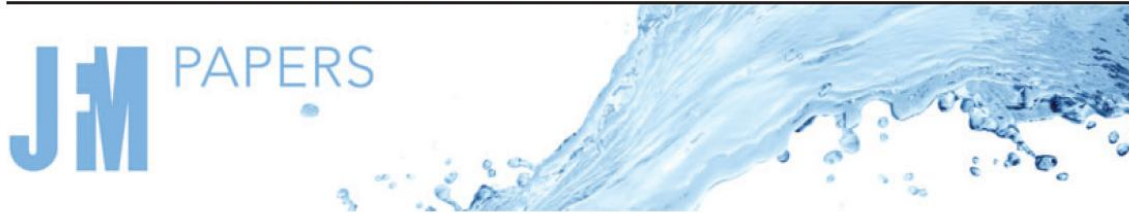
$$\frac{h_m}{R} \simeq \frac{4C_\tau}{\sqrt{\pi}} St^{-7/6}, \quad \text{with } C_\tau \simeq 12.4,$$

Capillary regime

$$\frac{h_m}{R} \simeq 8C_\tau^{2/3} We^{-1/3} St^{-10/9}.$$

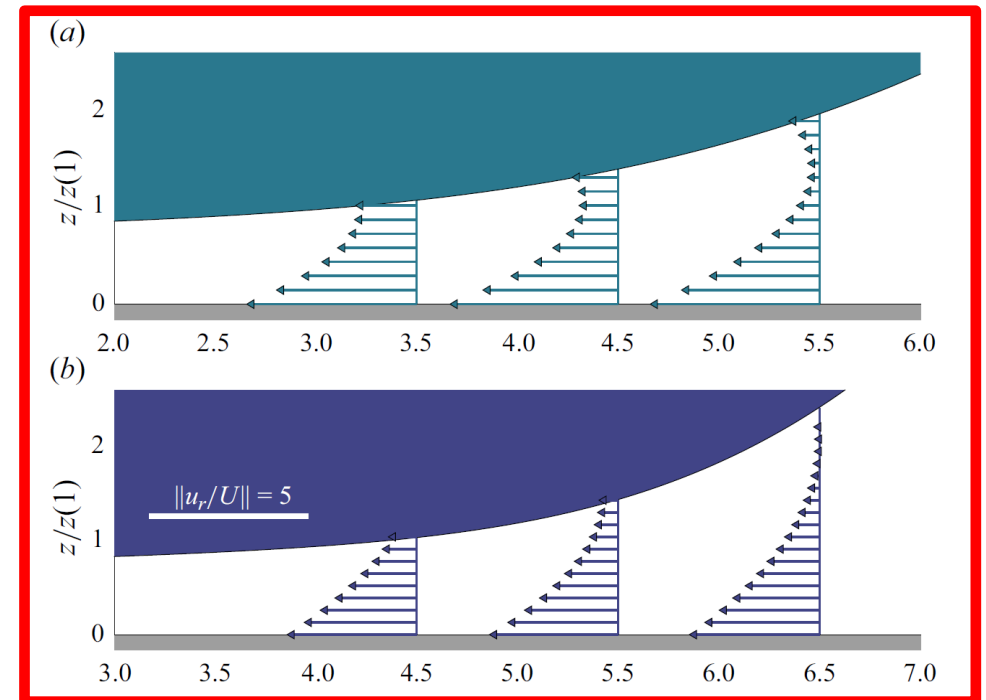
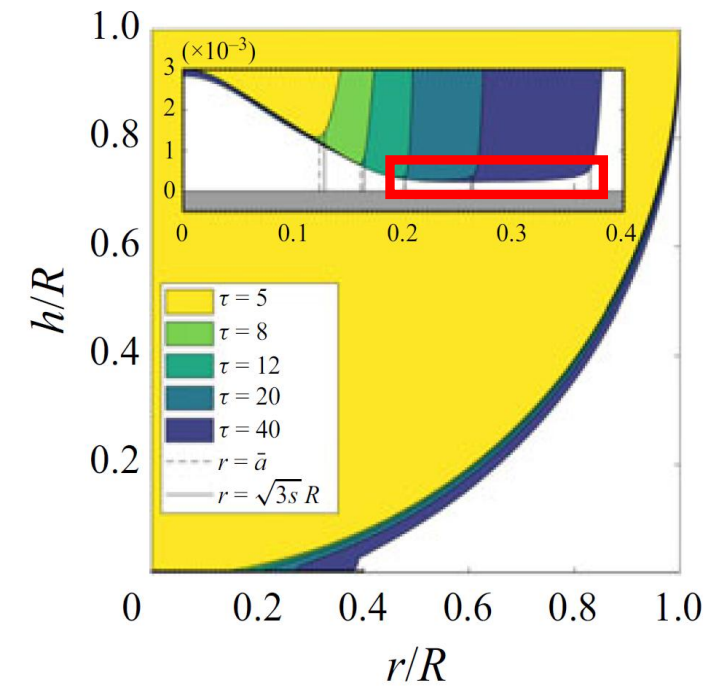
The purely numerical (not theoretical) results by Duchemin and Josserand published in PoF 2011 follow our prediction

J. Fluid Mech. (2024), vol. 980, A35, doi:10.1017/jfm.2024.20



The skating of drops impacting over gas or vapour layers

P. García-Geijo¹, G. Riboux¹ and J.M. Gordillo^{1,†}

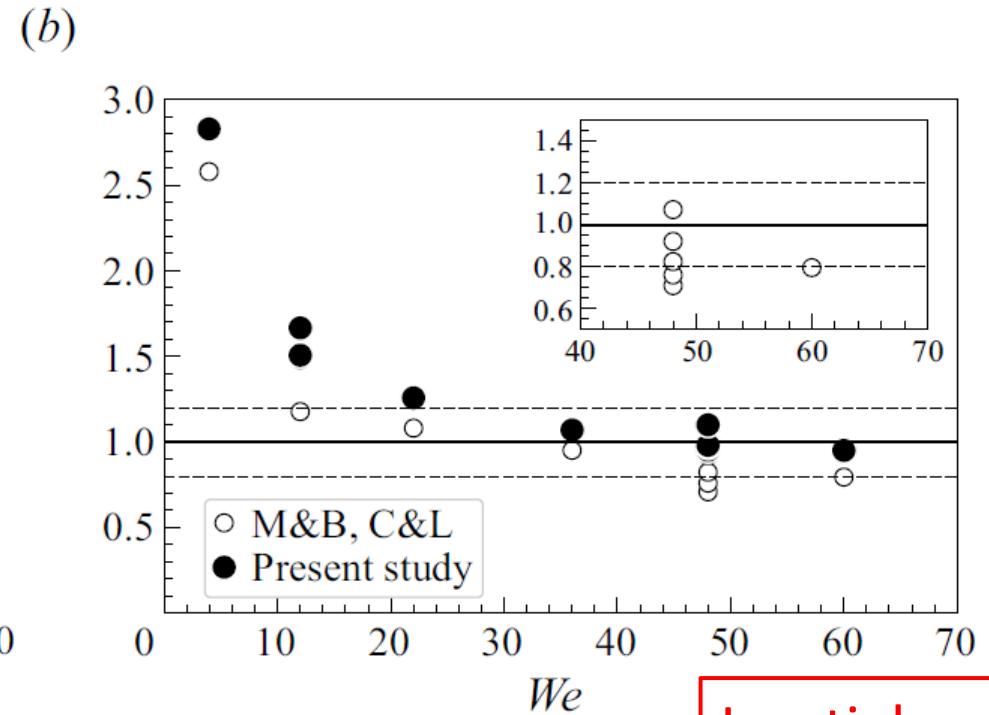
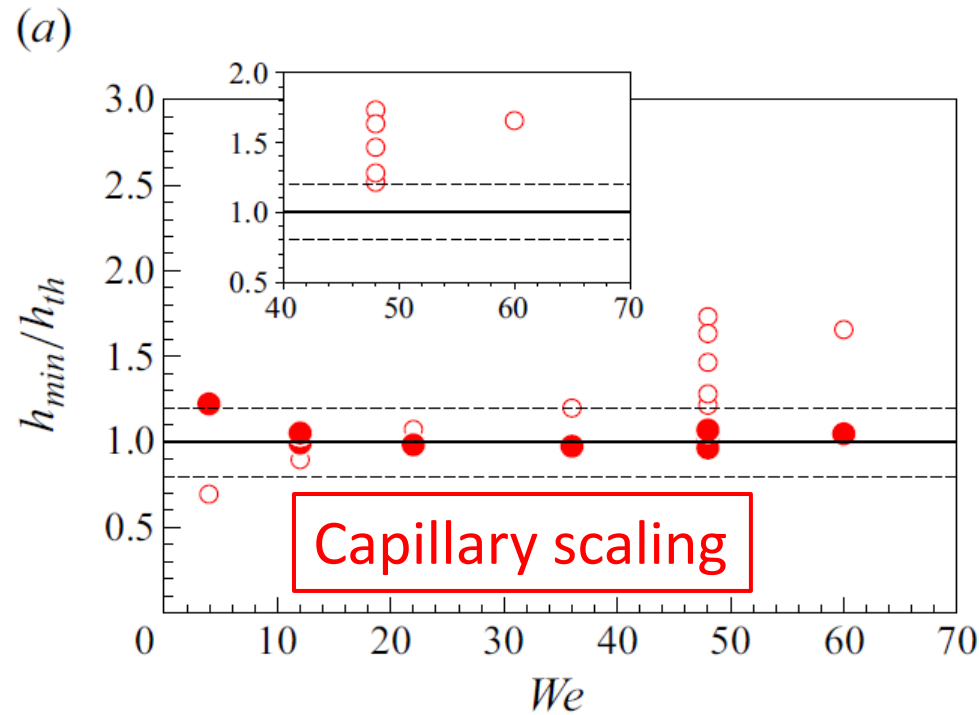


Mandre & Brenner and Chantelot and Lohse

- Capillary regime: $\frac{h_{mc,MB}}{R} \propto We^{-2/3} St^{-8/9}.$
- Inertial regime: $\frac{h_{mi,MB}}{R} \propto St^{-4/3}.$

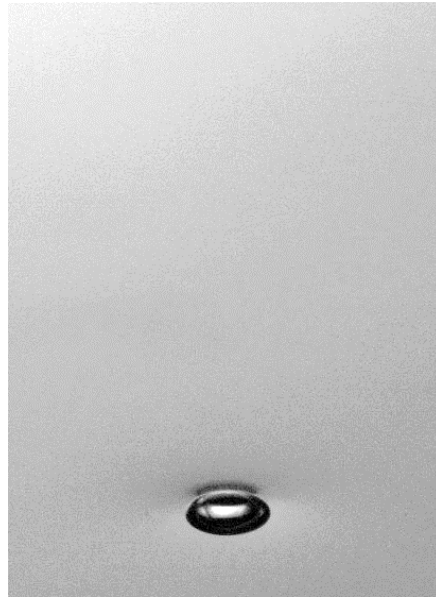
Gordillo and Riboux

- Capillary $\frac{h_m}{R} \simeq 8C_\tau^{2/3} We^{-1/3} St^{-10/9}.$
- Inertial $\frac{h_m}{R} \simeq \frac{4C_\tau}{\sqrt{\pi}} St^{-7/6}.$



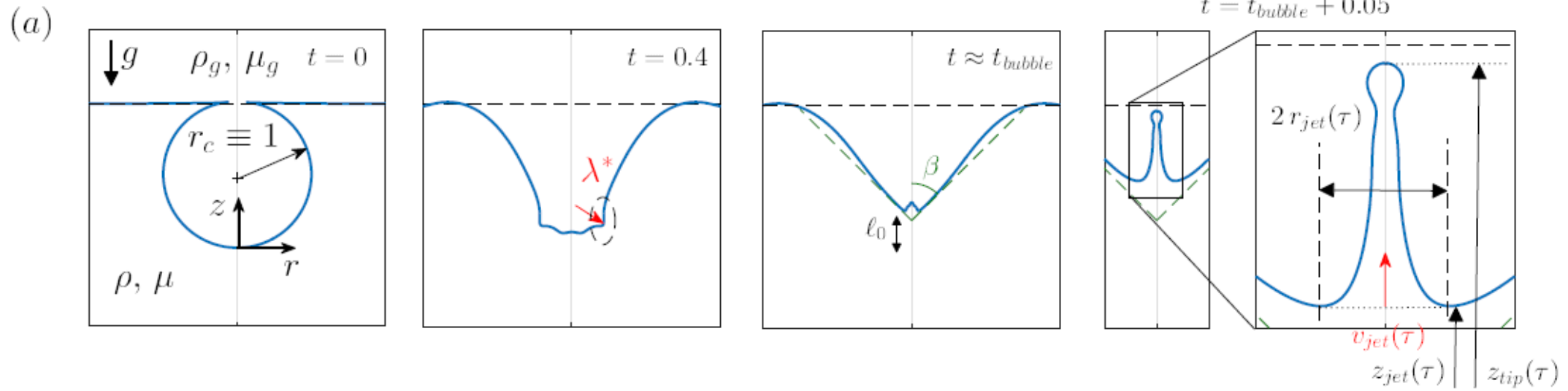
EXPERIMENTAL EVIDENCE AND NUMERICAL SIMULATIONS USING GERRIS BY POPINET

E Ghabache; A Antkowiak; C Josseland; T Séon; *Physics of Fluids* 2014, 26,



The bursting of a ~ 10 micron bubble in water generates a ~ 100 nm jet flowing with a speed larger than 100 m/s

**NUMERICAL SIMULATIONS
REVEAL THAT CAPILLARY
WAVES DEFORM THE INITIAL
SPHERICAL BUBBLE INTO A
TRUNCATED CONICAL SURFACE
AND A JET IS PRODUCED**

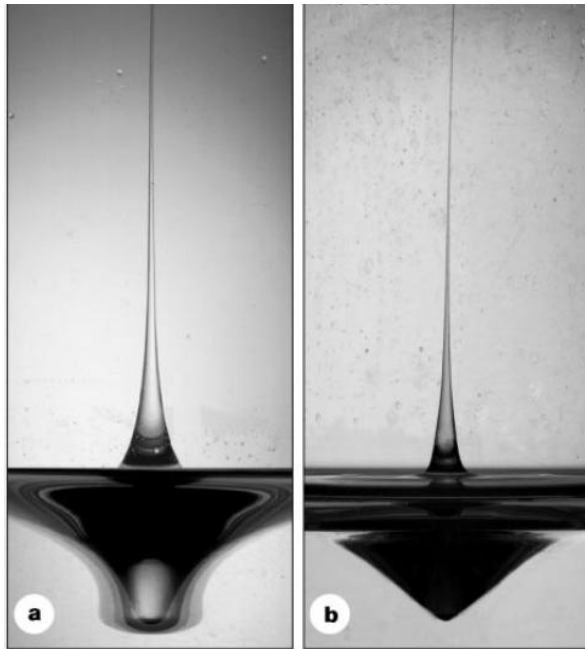


CLASSICAL DESCRIPTION OF THESE JETS: INERTIO-CAPILLARY BALANCE

Singularity dynamics in curvature collapse and jet eruption on a fluid surface

Benjamin W. Zeff*, Benjamin Kleber*, Jay Fineberg† & Daniel P. Lathrop*

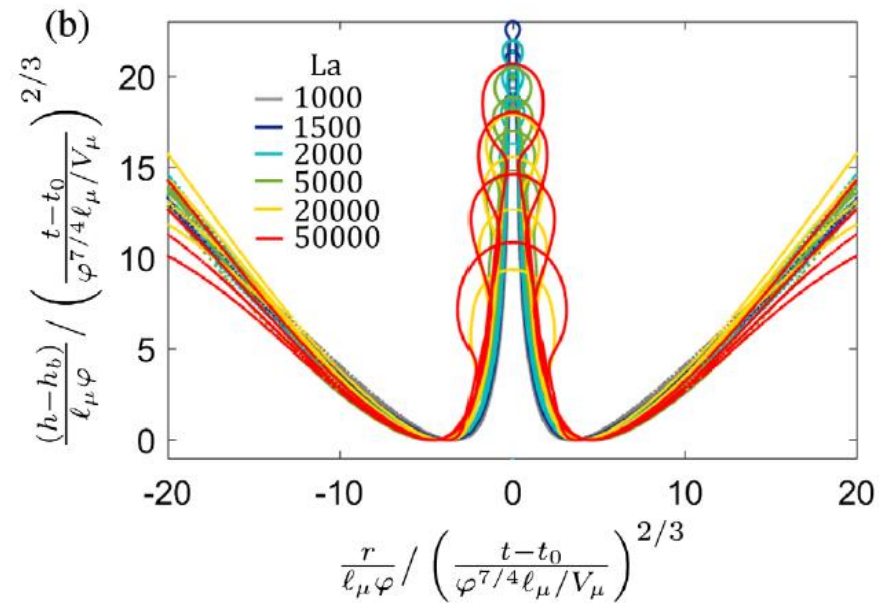
NATURE | VOL 403 | 27 JANUARY 2000 | www.nature.com



PHYSICAL REVIEW LETTERS 121, 144501 (2018)

Bubble Bursting: Universal Cavity and Jet Profiles

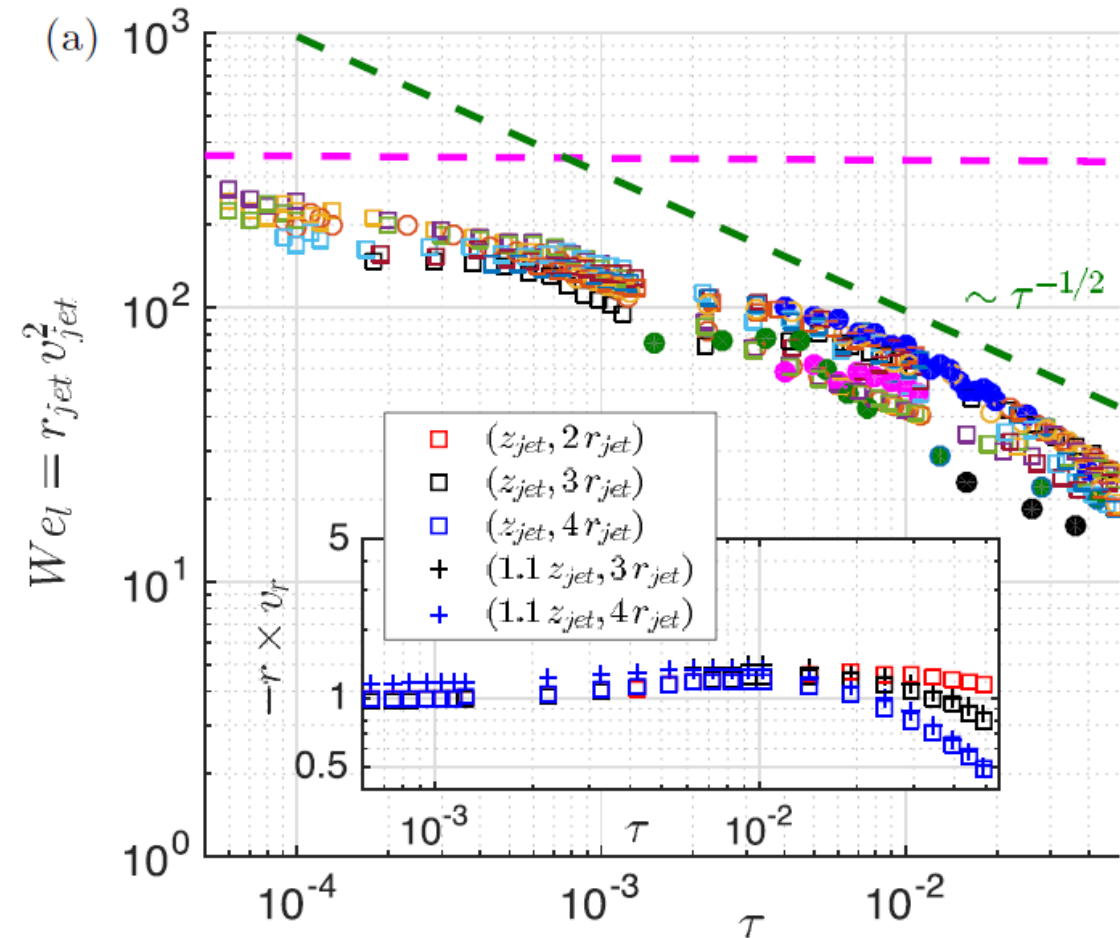
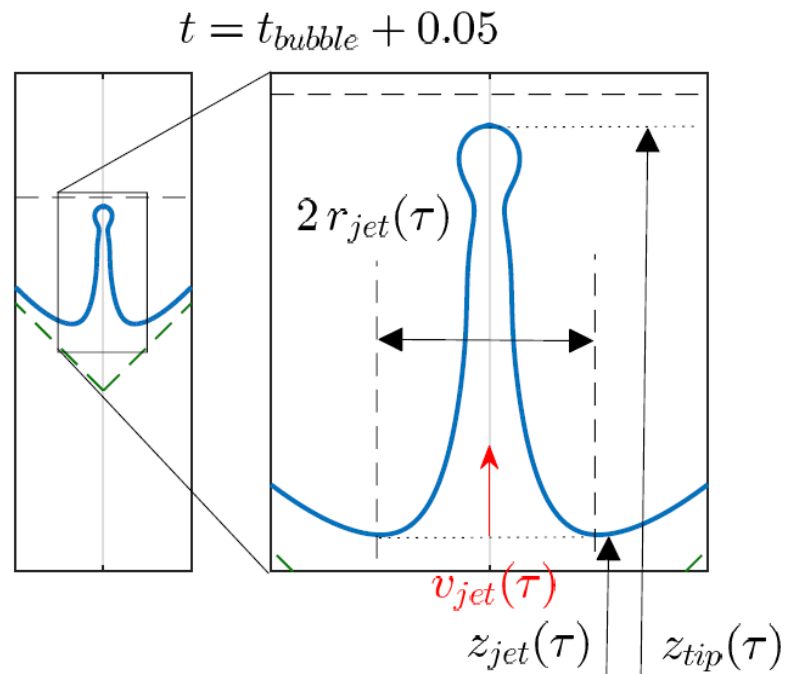
Ching-Yao Lai,¹ Jens Eggers,² and Luc Deike^{1,3,*}



**LONG JETS
ARE GENERATED,
AND THIS IS
INCONSISTENT
WITH A
DESCRIPTION IN
WHICH
CAPILLARY AND
INERTIA ARE IN
BALANCE:
ANYWAY, WE
CHECK IF THIS
BALANCE HOLDS**

$$\rho V_{\text{jet}}^2(T) \propto \sigma / R_{\text{jet}}(T) \longrightarrow We_l = \rho V_{\text{jet}}^2(\bar{T}) R_{\text{jet}}(\bar{T}) / \sigma \quad \text{CONSTANT}$$

... AS IT COULD HAVE BEEN ANTICIPATED IN VIEW OF THE FACT THAT THE JETS ARE LONG, THIS PHYSICAL PICTURE CANNOT BE CORRECT BECAUSE THE WEBER NUMBER IS MUCH LARGER THAN UNITY AND, MOST IMPORTANTLY IT DEPENDS ON TIME!

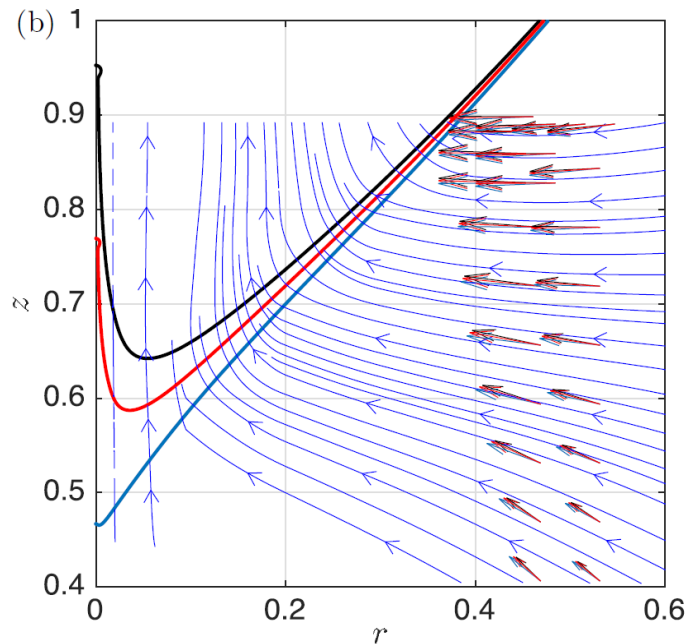


UNIFIED PURELY INERTIAL FRAMEWORK, WHICH DIVIDES THE JET EJECTION PROCESS IN TWO STAGES:

1.- ACCELERATION STAGE: FIXES THE VALUE OF THE FLOW RATE PER UNIT LENGTH DRIVING THE COLLAPSE OF THE CAVITY AND ALSO THE INITIAL SHAPE OF THE CAVITY, NAMELY

$$Q_{\infty} \quad \text{and} \quad r = r_s(\tau = 0, z)$$

$$Q_{\infty} \propto V_c R_b \quad \text{with} \quad \rho V_c^2 \sim \Delta p \Rightarrow Q_{\infty} \propto \left(\frac{\Delta p}{\rho} \right)^{1/2} R_b.$$



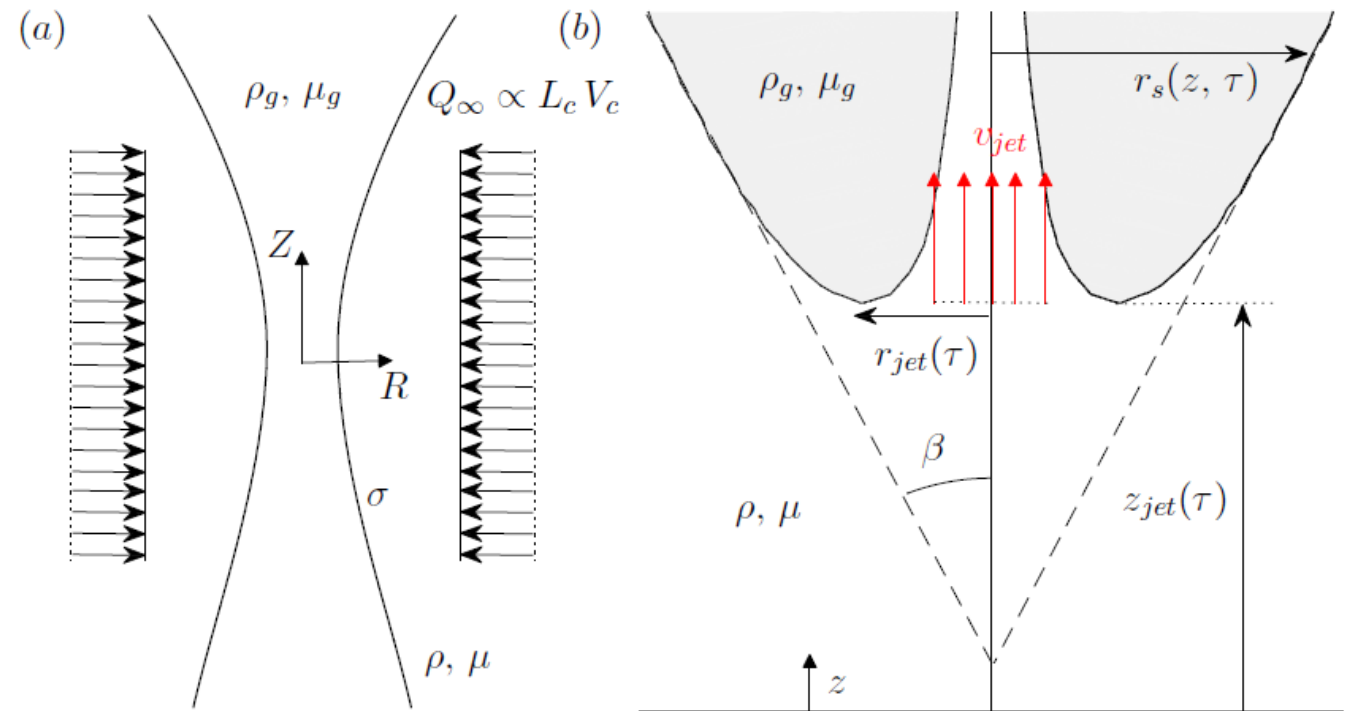
2.- JET EJECTION STAGE: THE FLOW RATE PER UNIT LENGTH REMAINS CONSTANT IN TIME BECAUSE OF THE LIQUID INERTIA AND THE SHORT TIME SCALE DURING WHICH THE JET IS EJECTED

JET EJECTION STAGE: ONCE THE FLOW RATE AND THE INITIAL SHAPE OF THE COLLAPSING CAVITY ARE KNOWN

$$Q_{\infty} \quad \text{and} \quad r = r_s(\tau = 0, z)$$

THE SPATIO-TEMPORAL EVOLUTION
OF THE JET AND OF THE DROPS
EJECTED CAN BE EXPLICITLY
CALCULATED IN TERMS OF

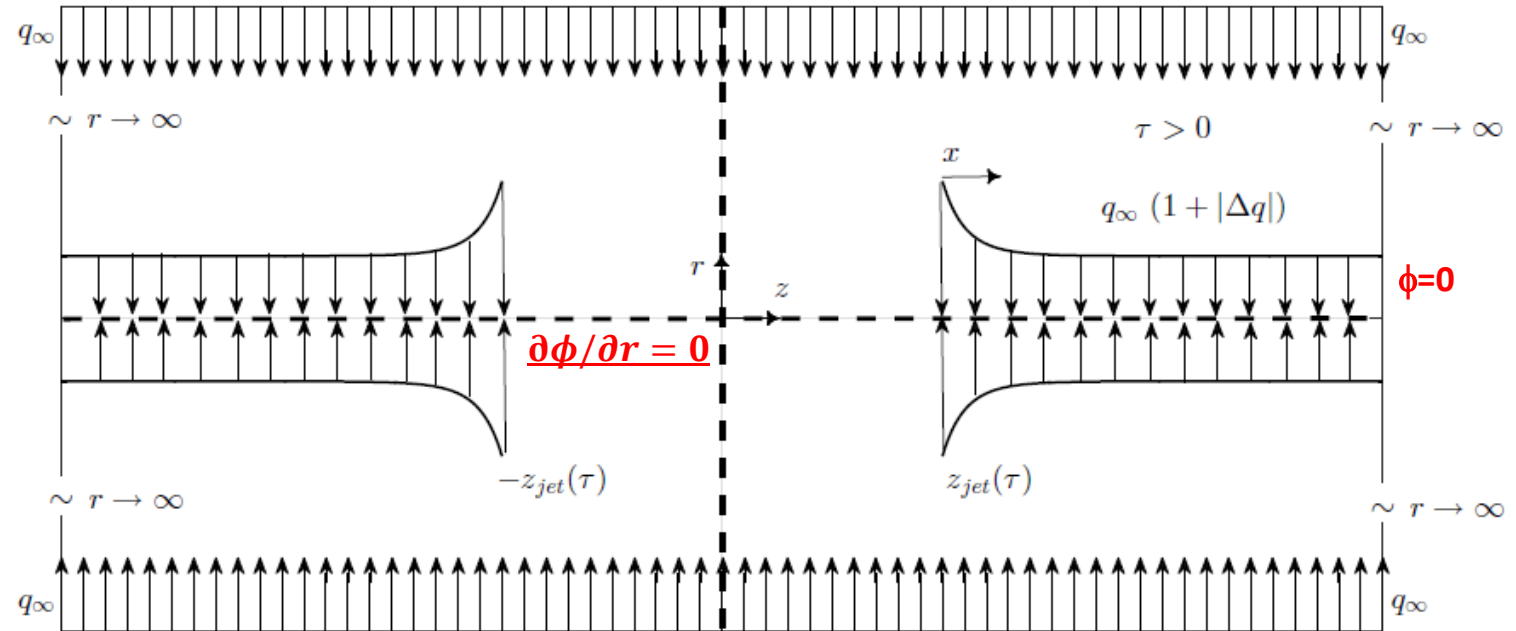
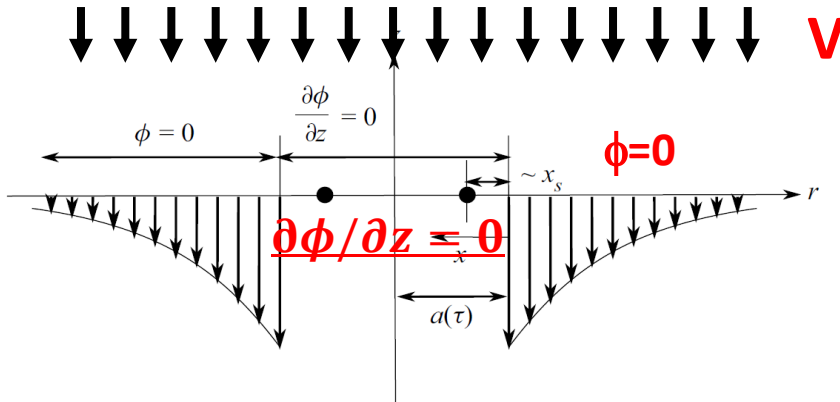
$r_{\text{jet}}(\tau)$, $z_{\text{jet}}(\tau)$ AND $v_{\text{jet}}(\tau)$



ANALYTICAL DESCRIPTION OF $r_{jet}(\tau)$, $z_{jet}(\tau)$ AND $u_{jet}(\tau)$ FOR THE CASE OF SLENDER CAVITIES: THE ANALOGY WITH A DROP IMPACTING A WALL IS THAT THE AXISYMMETRIC JET IS PRODUCED AS A CONSEQUENCE OF AN AXISYMMETRIC FLOW IMPACTING THE AXIS!

AXISYMMETRIC WORTHINGTON JET

DROP IMPACT



1.-SOLUTION OF THE LAPLACE EQUATION AS A DISTRIBUTION OF SINKS AT THE AXIS OF SYMMETRY
THE STRENGTH OF THE SINKS IS GIVEN BY THE CONDITION THAT THE AXIAL VELOCITIES ALONG THE
INTERFACE ARE ZERO

$$\int_{-z_{jet}}^{z_{jet}} \frac{(z - z_0) dz_0}{[(z - z_0)^2]^{3/2}} + \int_{z_{jet}}^{\infty} \frac{\Delta q(z_0) (z - z_0) dz_0}{[(z - z_0)^2]^{3/2}} + \int_{-\infty}^{-z_{jet}} \frac{\Delta q(-z_0) (z - z_0) dz_0}{[(z - z_0)^2]^{3/2}} = 0.$$

WE FOLLOW THE SAME STEPS AS FOR THE IMPACT OF A DROP ON A WALL

ANALYTICAL DESCRIPTION OF $r_{jet}(\tau)$, $z_{jet}(\tau)$ AND $v_{jet}(\tau)$

FOR THE CASE OF SLENDER CAVITIES

2.-KINEMATIC B.C IN ORDER TO DETERMINE WHEN THE INTERFACE REACHES THE AXIS OF SYMMETRY

$$\frac{dr_s}{d\tau} = v_r(r = r_s) = -q_\infty \frac{1 + |\Delta q|}{r_s} \Rightarrow -\frac{r_s^2(z = z_{jet})}{2q_\infty} = -\tau - \int_0^\tau |\Delta q(z = z_{jet}(\tau))| d\tau'.$$

$$\bar{x} = z_{jet}(\tau)/z'_{jet} - 1 \quad \text{with} \quad z'_{jet} = z_{jet}(\tau')$$

$$-\frac{r_s^2(z = z_{jet})}{2q_\infty} = -\tau - \int_\infty^0 |\Delta q(\bar{x})| \frac{d\tau'}{dz'_{jet}} \frac{dz'_{jet}}{d\bar{x}} d\bar{x}.$$

$$r_s^2(z = z_{jet}) = 2C^{-1} z_{jet}^n$$

$$\tau = A^{-1} z_{jet}^n$$

Conical slender cavities:

$$z_{jet} = \left(1 + 2 \int_0^\infty \frac{|\Delta q(\bar{x})|}{(1 + \bar{x})^3} d\bar{x} \right)^{1/2} (2q_\infty \tau / \tan^2 \beta)^{1/2} \simeq \frac{1.5}{\tan \beta} \sqrt{q_\infty \tau}$$

$$v_{jet} \simeq 2 \frac{dz_{jet}}{d\tau} \simeq \frac{1.5}{\tan \beta} \sqrt{\frac{q_\infty}{\tau}},$$

Parabolic cavities:

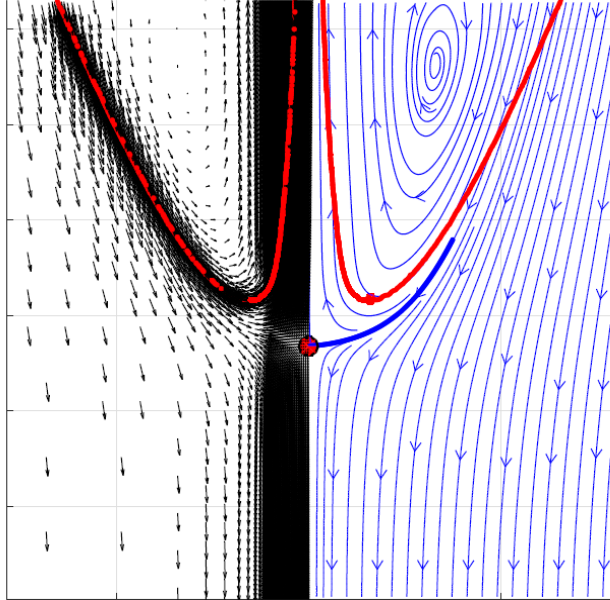
$$z_{jet} = 1.25 (2r_c)^{1/2} (q_\infty \tau)^{1/4} \quad \text{and} \quad v_{jet} = 0.625 q_\infty (2r_c)^{1/2} (q_\infty \tau)^{-3/4}$$

WE FOLLOW THE SAME STEPS AS FOR THE IMPACT OF A DROP ON A WALL

ANALYTICAL DESCRIPTION OF $r_{jet}(\tau)$, $z_{jet}(\tau)$ AND $v_{jet}(\tau)$

FOR THE CASE OF SLENDER CAVITIES

3.-EULER-BERNOULLI EQUATION IN THE FRAME OF REFERENCE MOVING WITH THE VELOCITY AT WHICH THE CAVITY COLLAPSES IN THE VERTICAL DIRECTION: THE MODULUS OF THE VELOCITY IS CONSTANT ALONG THE FREE SURFACE IN THE MOVING FRAME OF REFERENCE



$$v_{jet} \simeq 2 \frac{dz_{jet}}{d\tau} \simeq \frac{2Cq_{\infty}}{n} \left(1 + n \int_0^{\infty} \frac{|\Delta q(\bar{x})|}{(1+\bar{x})^{n+1}} d\bar{x} \right)^{1/n} (Cq_{\infty}\tau)^{(1-n)/n}.$$

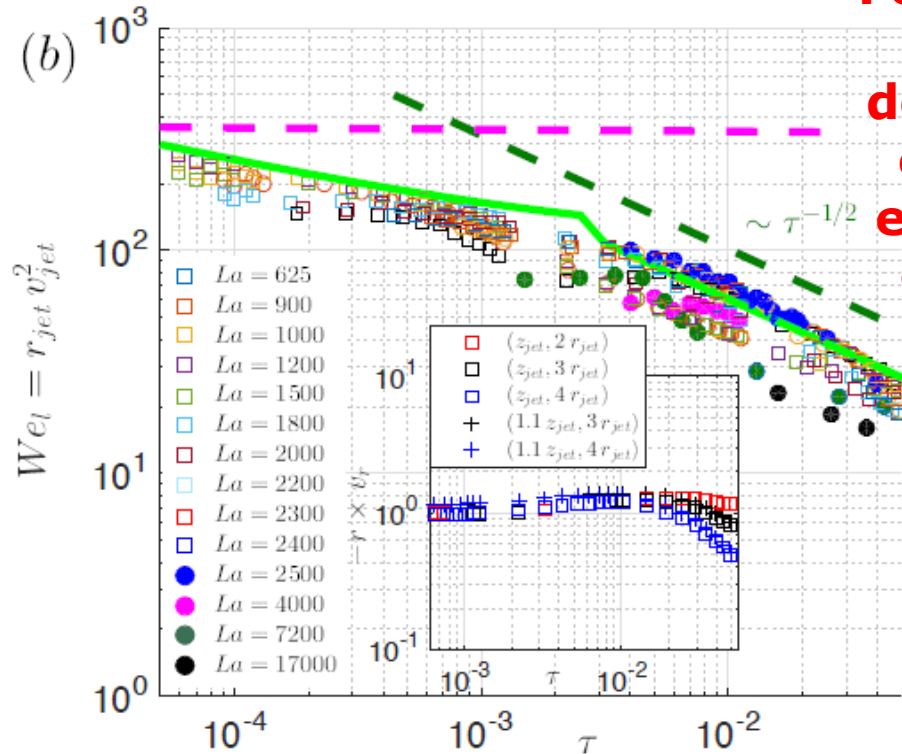
4.-THE FLOW RATE IN THE JET MUST BE THE ONE IMPOSED AT THE FAR FIELD OF THE INNER REGION, NAMELY, THE FLOW RATE OF THE OUTER REGION AT THE BASE OF THE JET

$$2\pi \int_{z_{jet}}^{z_{jet}+r_{jet}} q_{\infty} (1 + |\Delta q(z)|) dz \approx 2\pi r_{jet}^2 \frac{dz_{jet}}{d\tau} \Rightarrow r_{jet} \frac{dz_{jet}}{d\tau} \simeq 1.7q_{\infty},$$

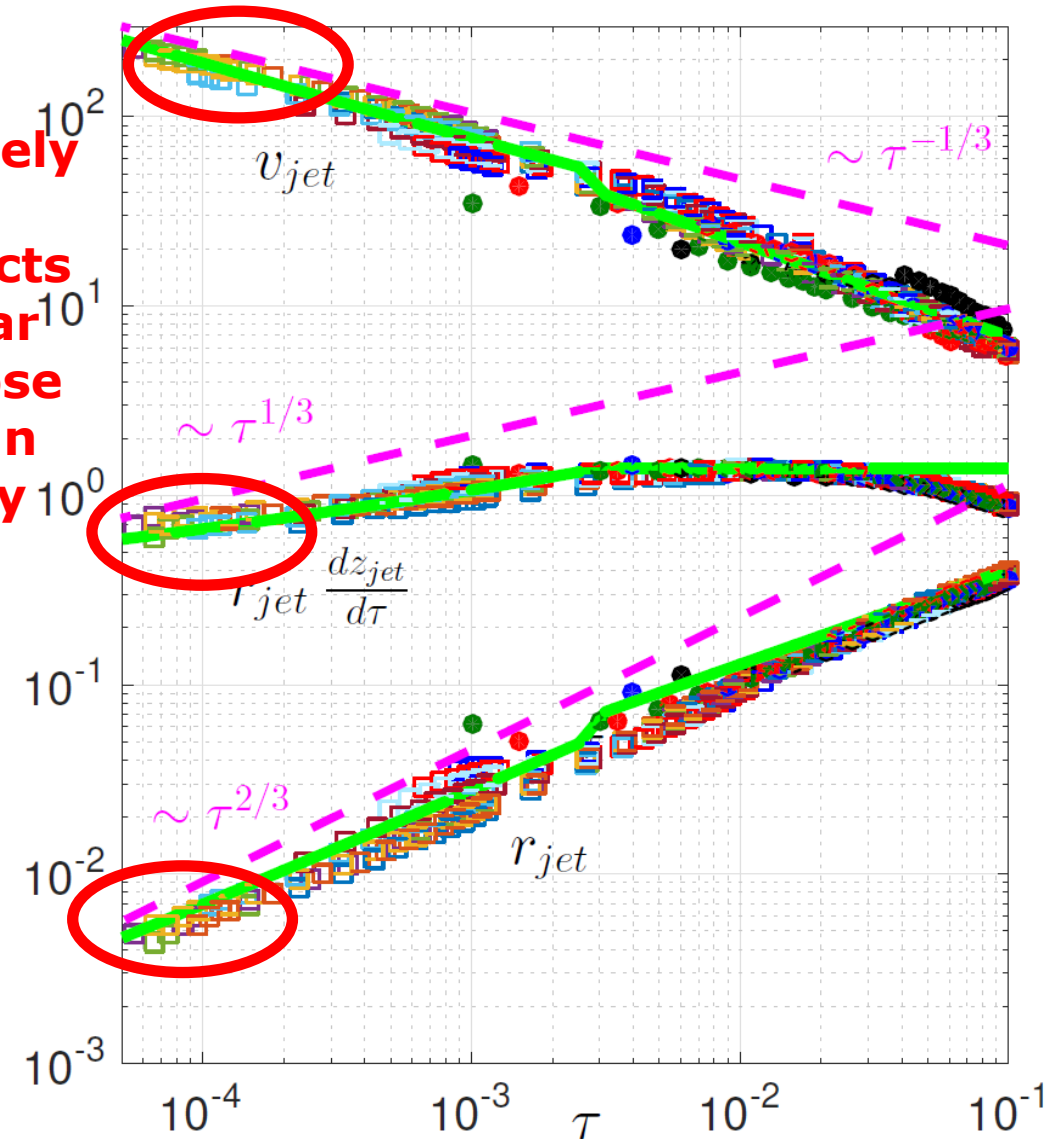
COMPARISON BETWEEN NUMERICAL SIMULATIONS AND PREDICTIONS

BUBBLE BURSTING JETS: CONICAL CAVITIES

$$v_{jet} = \frac{1.5K(\beta)}{\tan \beta} \sqrt{\frac{q_{\infty}(r_{jet})}{\tau}}, \quad r_{jet} v_{jet} \simeq 3.4 q_{\infty}$$



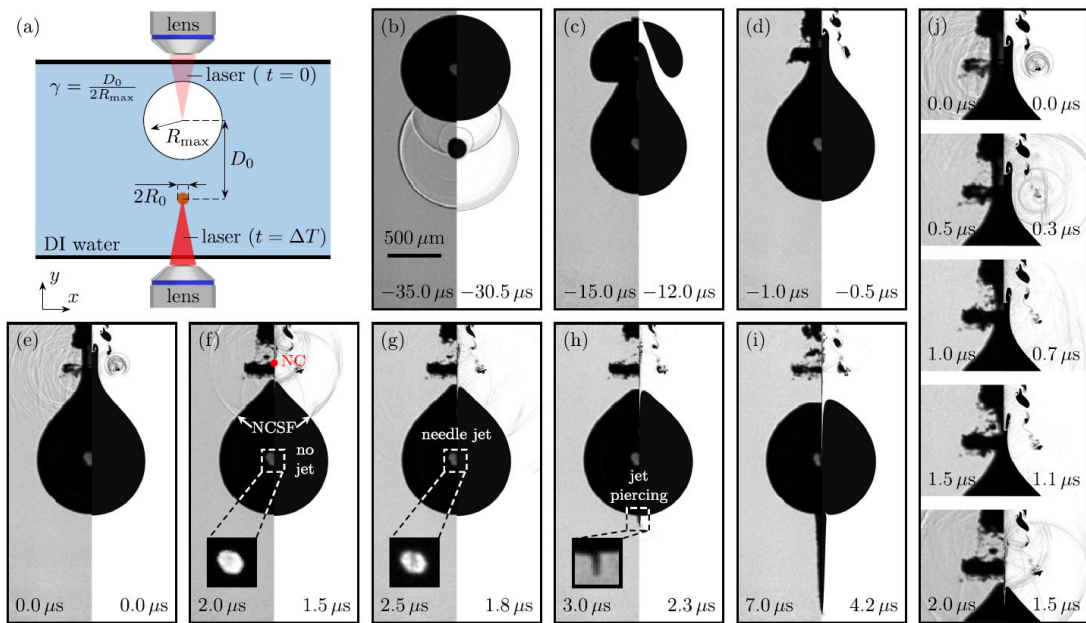
For $\tau \ll 1$, the purely inertial description predicts extremely similar exponents to those characterizing an Inertio-Capillary balance



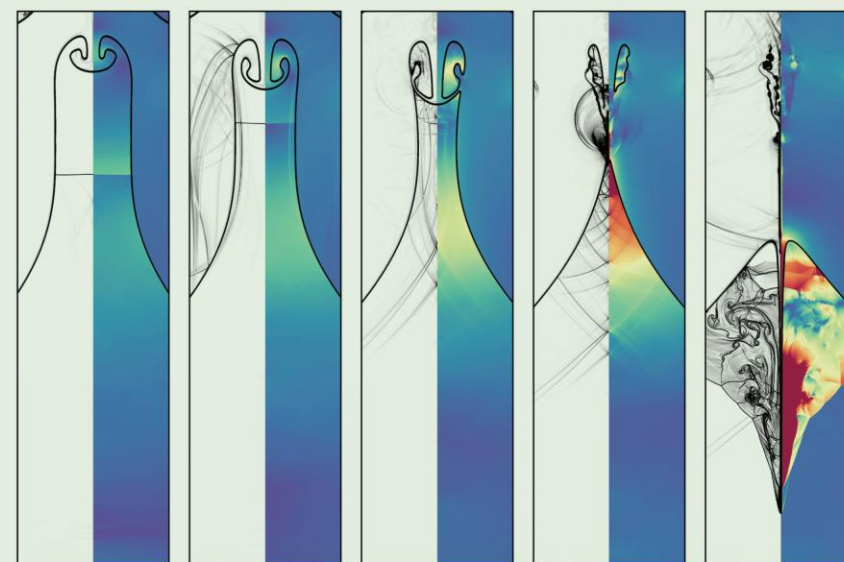
Pink lines, inertio-capillary balance:

C.-Y. Lai, J. Eggers, and L. Deike,
Phys. Rev. Lett. **121**, 144501 (2018).

PARABOLIC CAVITIES...



Jet speed exceeds 1000 m/s



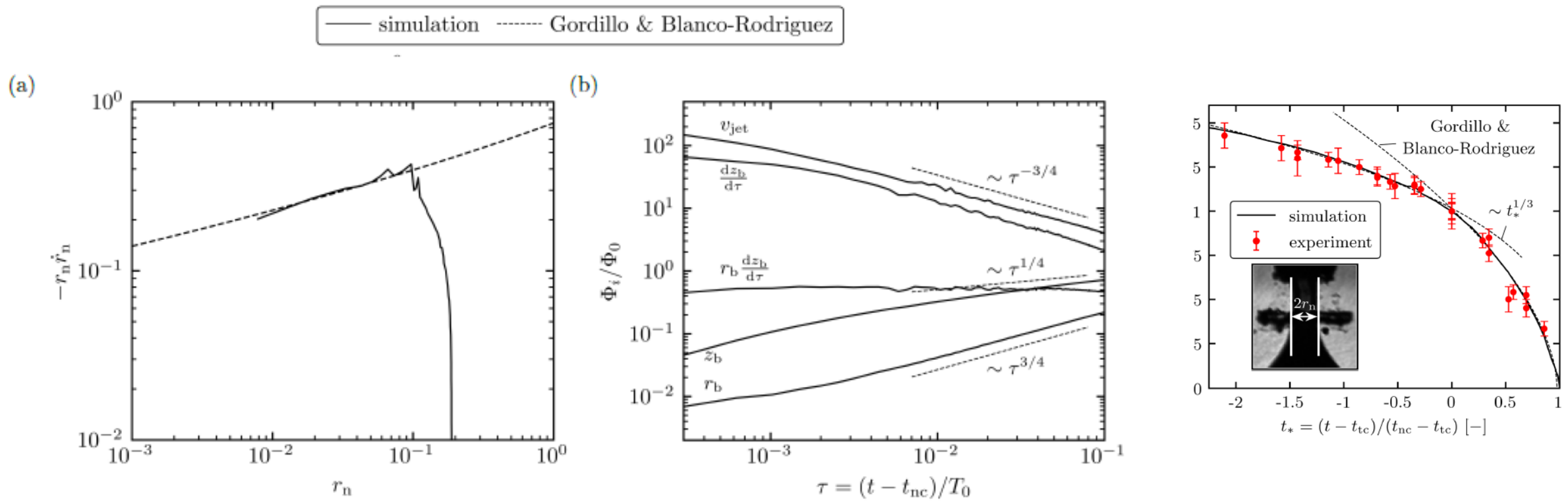
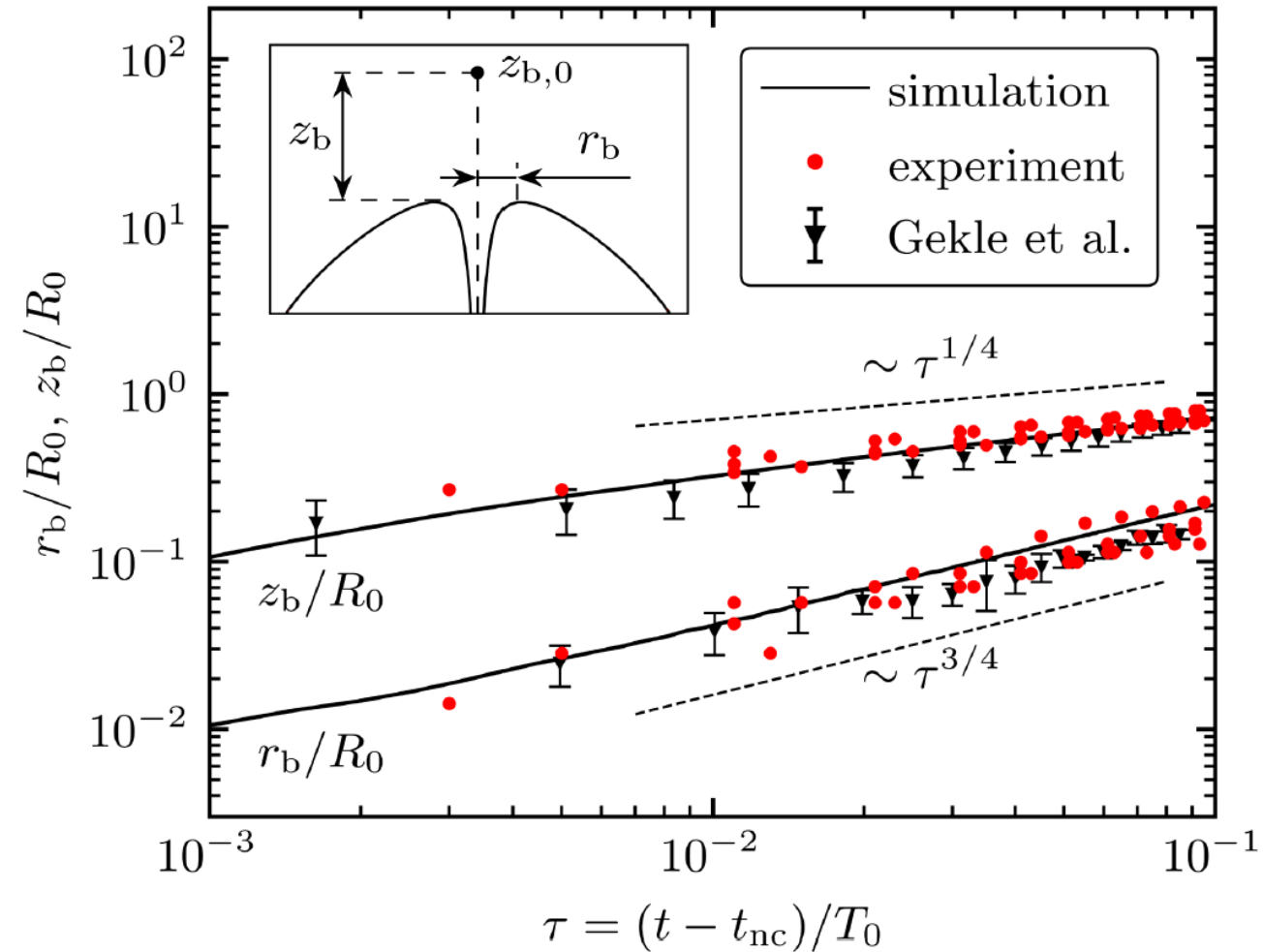
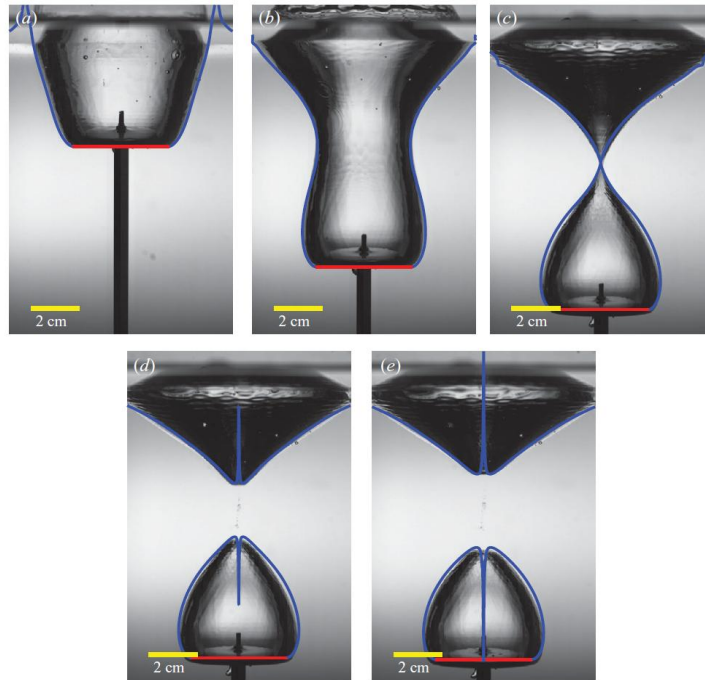
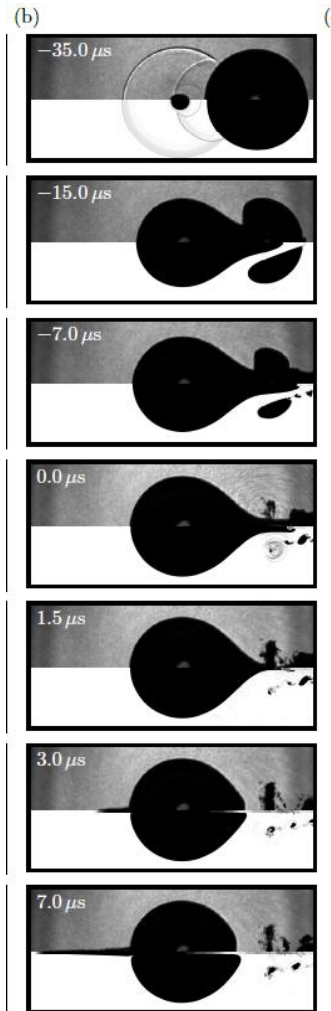


FIG. 3. **Comparison of neck collapse and jet ejection between simulation and theory.** (a) Non-dimensional flow rate at the neck apex, $r_n \dot{r}_n$, over the neck radius, r_n , during the collapse of the parabolic neck. (b) Non-dimensional jet characteristics of the radial jet base, r_b , the axial jet base, z_b , the jet flow rate, $r_b dz_b/d\tau$, and the jet base velocity, v_{jet} . In both plots, the solid line corresponds to the simulation, and the dashed line represents the theoretical predictions of Gordillo and Blanco-Rodríguez [1, 2].

WORTHINGTON JETS FOR THE CASE OF PARABOLIC CAVITIES

$$z_{jet} = 1.25 (2r_c)^{1/2} (q_\infty \tau)^{1/4} \quad \text{and} \quad v_{jet} = 0.625 q_\infty (2r_c)^{1/2} (q_\infty \tau)^{-3/4}$$



$$2\pi \int_{z_{jet}}^{z_{jet}+r_{jet}} q_\infty (1 + |\Delta q(z)|) dz \approx 2\pi r_{jet}^2 \frac{dz_{jet}}{d\tau} \Rightarrow r_{jet} \frac{dz_{jet}}{d\tau} \simeq 1.7 q_\infty,$$



MORE DETAILS IN

PHYSICAL REVIEW FLUIDS 8, 073606 (2023)

Theory of the jets ejected after the inertial collapse of cavities with applications to bubble bursting jets

José M. Gordillo * and Francisco J. Blanco-Rodríguez 

*Área de Mecánica de Fluidos, Departamento de Ingeniería Aeroespacial y Mecánica de Fluidos,
Universidad de Sevilla, 41092 Sevilla, Spain*

THE SPLASH OF A DROP IMPACTING A WALL AND THE EJECTION OF WORTHINGTON JETS CAN BE DESCRIBED USING THE SAME THEORETICAL FRAMEWORK. IN THE CASE OF DROPS, THE NON IMPENETRABILITY CONDITION IS IMPOSED AT AN HORIZONTAL PLANE I.E, THE WETTED AREA OF THE SOLID, WHEREAS FOR THE CASE OF WORTHINGTON JETS, THE IMPENETRABILITY CONDITION FOR THE RADIAL FAR FIELD FLOW IS IMPOSED AT THE AXIS OF SYMMETRY.

THESE TWO DIFFERENT PHYSICAL SITUATIONS ARE, CONCEPTUALLY, THE SAME MATHEMATICAL PROBLEM BUT WITH A DIFFERENT TYPE OF SYMMETRY.

THANK YOU FOR YOUR ATTENTION!

EJECTION TIME AND THE SPLASH CRITERION

PRL 113, 024507 (2014)

PHYSICAL REVIEW LETTERS

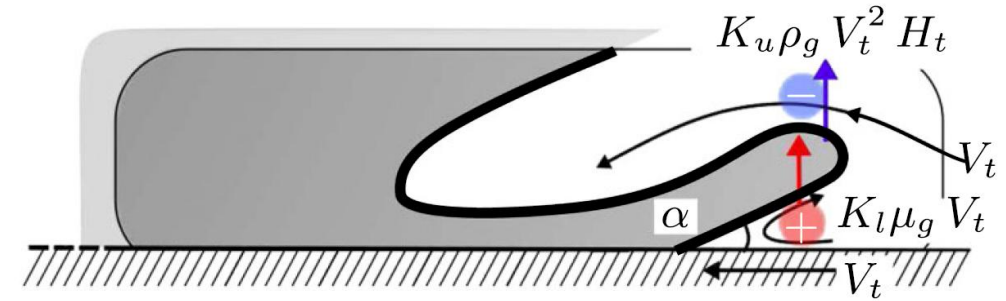
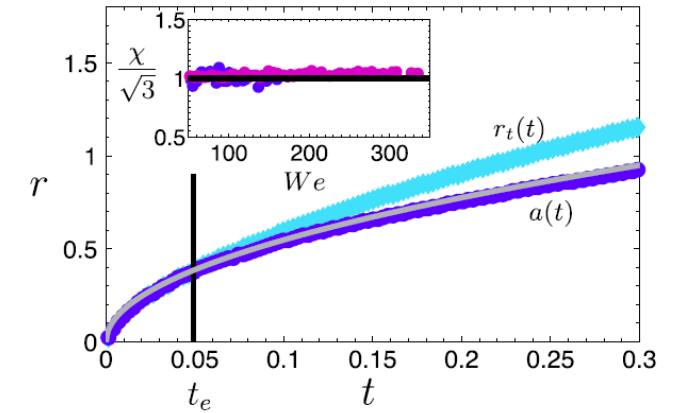
week ending
11 JULY 2014



Experiments of Drops Impacting a Smooth Solid Surface: A Model of the Critical Impact Speed for Drop Splashing

Guillaume Riboux and José Manuel Gordillo*

THE EJECTION TIME IS THE INSTANT AT WHICH THE DECELERATION OF THE TIP OF THE LAMELLA CAUSED BY CAPILLARITY AND VISCOSITY IS SMALLER THAN THE ONE ASSOCIATED WITH THE WETTING OF THE SOLID, \ddot{a}



$$\frac{\sqrt{3}}{2} \text{Re}^{-1} t_e^{-1/2} + \text{Re}^{-2} \text{Oh}^{-2} = 1.1 t_e^{3/2}$$

THE SPLASH TRANSITION TAKES PLACE WHEN THE VERTICAL VELOCITY OF THE EDGE OF THE LAMELLA CAUSED BY THE LIFT FORCE IS LARGER THAN THE RADIAL VELOCITY CAUSED BY THE CAPILLARY RETRACTION OF THE EDGE OF THE LAMELLA

$$\rho H_t^2 \dot{V}_v \propto \ell \longrightarrow V_v(T_e) = C_v \sqrt{\ell / (\rho H_t)}$$

$$V_r = \sqrt{2\sigma / \rho H_t}$$

$$\beta = \frac{V_v}{V_r} = \left(\frac{K_l \mu_g V_t + K_u \rho_g V_t^2 H_t}{2\sigma} \right)^{1/2}$$

Axisymmetric bubble collapse in a quiescent liquid pool. I. Theory and numerical simulations

Cite as: Phys. Fluids **20**, 112103 (2008); <https://doi.org/10.1063/1.3009297>

Submitted: 06 June 2008 . Accepted: 12 September 2008 . Published Online: 18 November 2008

J. M. Gordillo

$$\ln \left(\frac{r_0}{2r_c} \right) \frac{d \ln \bar{q}}{ds} - 1 + \gamma \frac{\rho_g}{\rho} \frac{p}{[r_0/(2r_c)]} + \frac{4Oh}{\bar{q} r_0 \dot{r}_0(0)} = 0$$

$$s = -\ln(r_0)$$

$$\ln \left(\frac{r_0}{2r_c} \right) \frac{d}{ds} \left[\ln \left(\frac{r_0}{2r_c} \right) \right] - 1 + \frac{1}{2} \frac{\rho_g}{\rho} \frac{p}{[r_0/(2r_c)]} + \frac{4Oh}{\bar{q} r_0 \dot{r}_0(0)} = 0,$$

$$\bar{q} = \frac{r_0 \dot{r}_0}{r_0 \dot{r}_0(0)} \quad \text{and} \quad \frac{dt}{ds} = -\frac{e^{-2s}}{r_0 \dot{r}_0},$$

$$\frac{d}{ds} \left[\ln \left(\frac{r_0}{2r_c} \frac{1}{\bar{q}} \right) \right] = 0 \Rightarrow \bar{q} = \frac{r_0/(2r_c)}{[r_0/(2r_c)(0)]}.$$

$$\ln \left(\frac{r_0}{2r_c} \right) \frac{d}{ds} \left[\ln \left(\frac{r_0}{2r_c} \right) \right] - 1 = 0 \Rightarrow \frac{d}{ds} \left[\ln \left(\frac{r_0}{2r_c} \right) \right]^2 - 2 = 0 \Rightarrow$$

$$\left[\ln \left(\frac{r_0}{2r_c} \right) \right]^2 - \left[\ln \left(\frac{r_0(0)}{2r_c(0)} \right) \right]^2 = 2(s - s(0)) = -2 \ln \left(\frac{r_0}{r_0(0)} \right)$$

$$r_0 = r_0(0) e^{(1/2)[\ln(r_0(0)/(2r_c(0)))]^2} e^{-(1/2)[\ln(r_0/(2r_c))]^2}$$

$$q(t) = -r_0 \dot{r}_0 = \frac{-r_0 \dot{r}_0(0)}{[r_0/(2r_c)(0)]} \times \exp \left(-\sqrt{\left[\ln \left(\frac{r_0(0)}{2r_c(0)} \right) \right]^2 - \ln \left(\frac{r_0}{r_0(0)} \right)^2} \right)$$

COMPARISON BETWEEN NUMERICAL SIMULATIONS AND PREDICTIONS, BUBBLE BURSTING JETS-IV

$$v_{jet} = \frac{1.5K(\beta)}{\tan \beta} \sqrt{\frac{q_{\infty}(r_{jet})}{\tau}}, \quad r_{jet} v_{jet} \simeq 3.4 q_{\infty}$$

If $r_{jet} \leq 0.05$ $q_{\infty}(r_{jet}) = -\frac{r_0 \dot{r}_0(0)}{[r_0/(2r_c)(0)]} \times \exp \left(-\sqrt{\left[\ln \left(\frac{r_0(0)}{2r_c(0)} \right) \right]^2 - \ln \left(\frac{r_{jet}}{r_0(0)} \right)^2} \right)$

If $r_{jet} > 0.05$ $q_{\infty} = 0.82$.

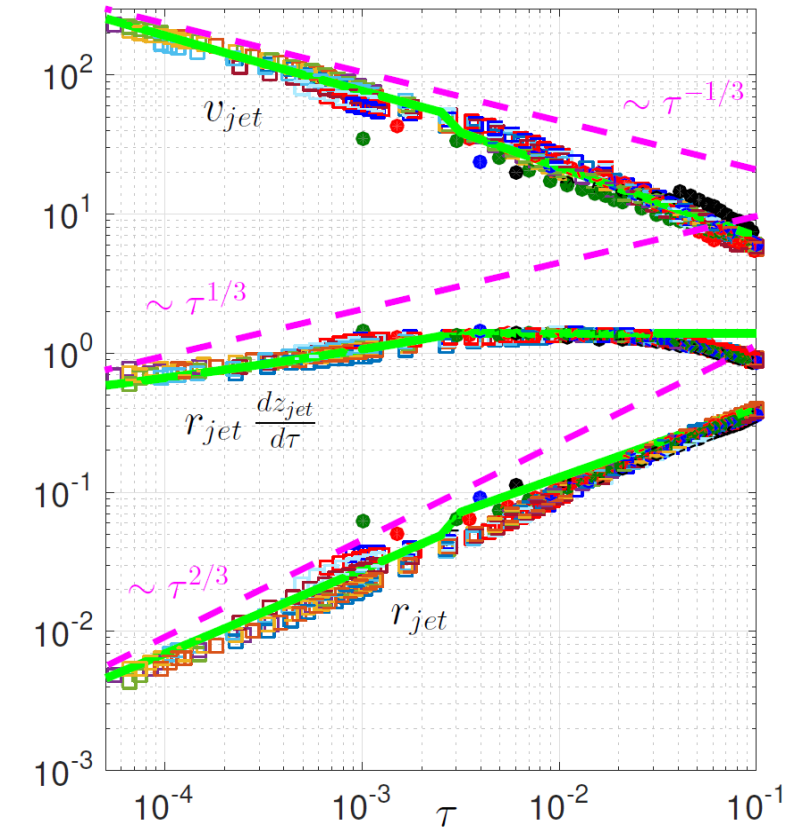
**Initial values of the jet radius and velocity
when a bubble is entrapped: limited by viscosity if
axisymmetry is preserved**

$$Re_l = Oh^{-1} r_{jet} v_{jet} \gtrsim O(1) \Rightarrow q_{\infty} \geq K Oh$$

$$r_{jet0}(La < 2500) = r_0(0) \times$$

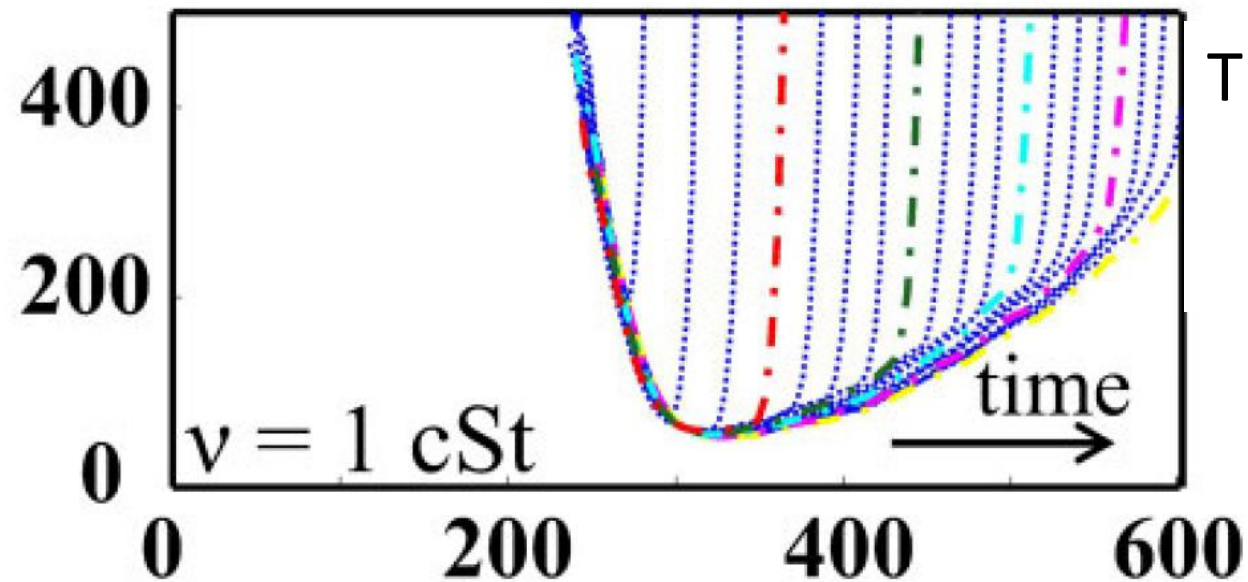
$$\exp \left(-\frac{1}{2} \left[\left[\ln \left(\frac{-K Oh r_0(0)}{(2r_c r_0 \dot{r}_0)(0)} \right) \right]^2 - \left[\ln \left(\frac{r_0(0)}{2r_c(0)} \right) \right]^2 \right] \right)$$

$$v_{jet0}(La < 2500) = \frac{3.4 q_{\infty}(r_{jet0})}{r_{jet0}} = \frac{3.4 K Oh}{r_{jet0}(La < 2500)} \quad (6)$$



Lift-Off Instability During the Impact of a Drop on a Solid Surface

John M. Kolinski,^{1,2} L. Mahadevan,^{1,3} and Shmuel M. Rubinstein^{1,2,*}



They reported experiments showing that the spreading front lifts-off away from the surface

The lift-off instability, even when the liquid evaporates, can also be explained using the same framework because

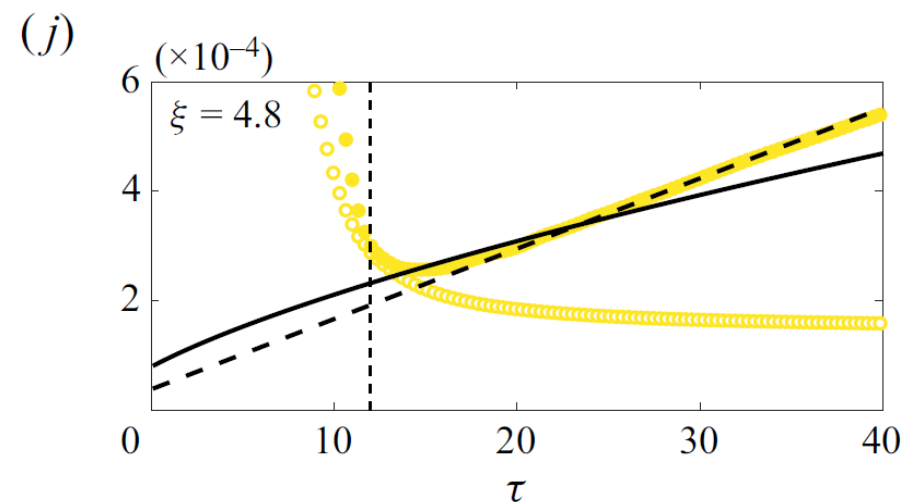
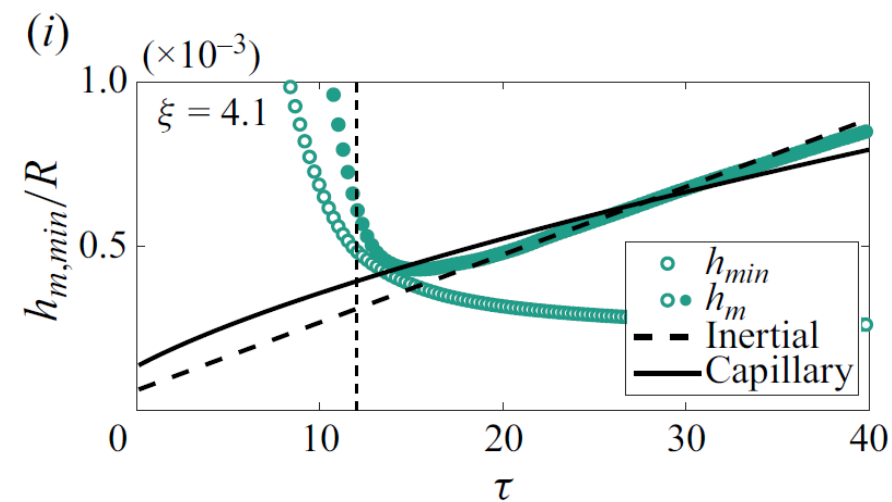
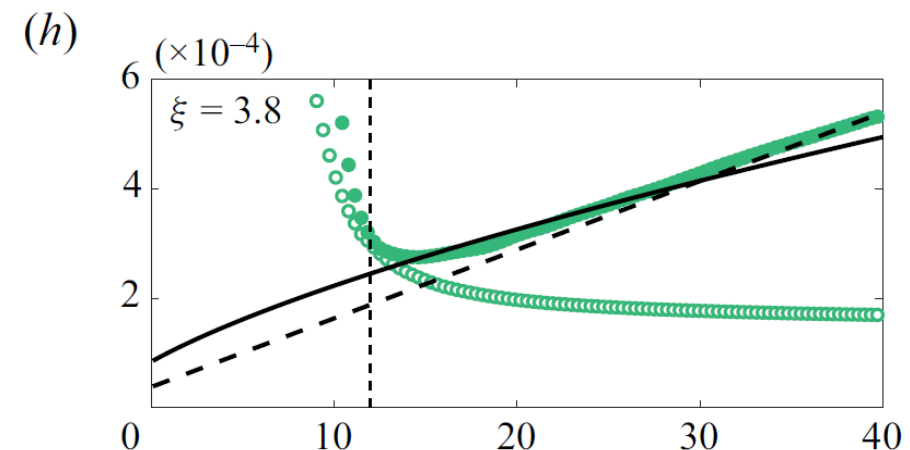
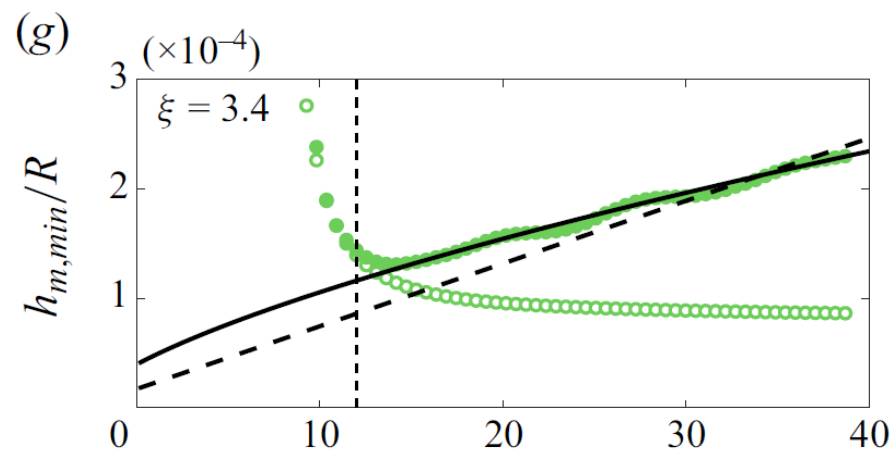
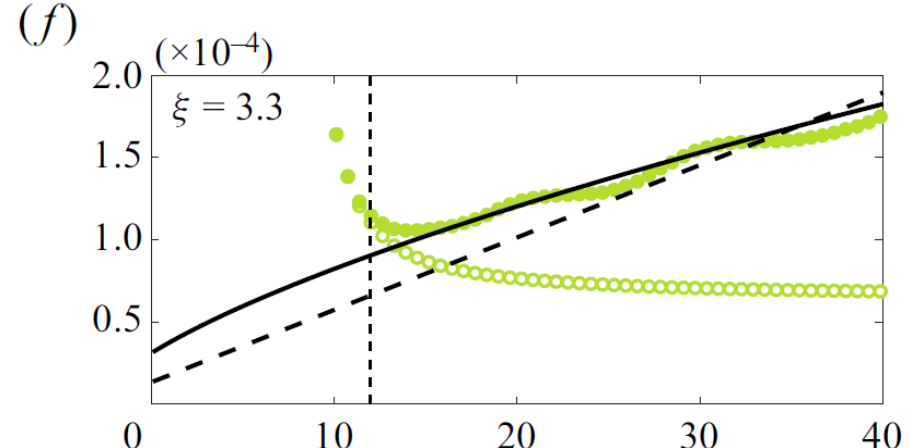
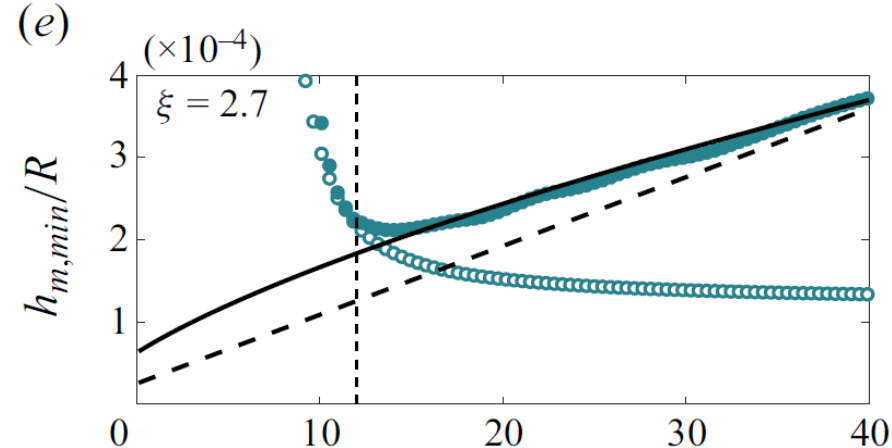
$$\ell \, dh_m/dt \ll V_m h_m$$

Then, mass conservation at the thin film implies that

$$-\frac{h_m^3}{12\mu_v} \frac{\partial p}{\partial r} - \frac{V_m h_m}{2} \approx \frac{k_v \Delta T}{\rho_v \mathcal{L}} \frac{\ell}{h_m},$$

$$\left. \begin{aligned} \frac{h_{m,c}}{R} &= 2.42 y^{2/3} (\tau + 3)^{2/3} We^{-1/3} St^{-10/9}. \\ \frac{h_{m,i}}{R} &= 0.48 y^{1/2} (\tau + 3) St^{-7/6}. \end{aligned} \right\} \quad \begin{aligned} y &= 3 \left(\frac{\mu_v}{\mu_a} \right) \left[1 + \sqrt{1 + \frac{2\beta^*}{3} \left(\frac{\mu_a}{\mu_v} \right)} \right]. \\ \beta^* &= \beta \left(\frac{\rho}{\rho_v} \right) \left(\frac{\mu_v}{\mu_a} \right), \quad \text{where } \beta = \frac{k_v \Delta T}{\mu_v \mathcal{L}}. \end{aligned}$$

**Comparison
between
the calculated time-
varying
minimum gas film
thickness
and the predictions
for different values
of We and St**



INFLUENCE OF SUBSTRATE ROUGHNESS AND WETTABILITY

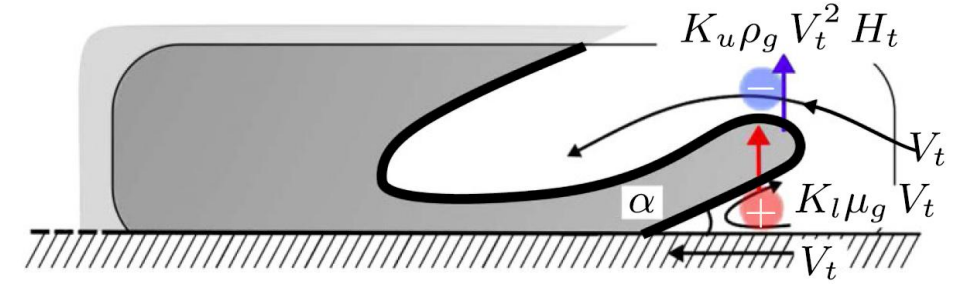
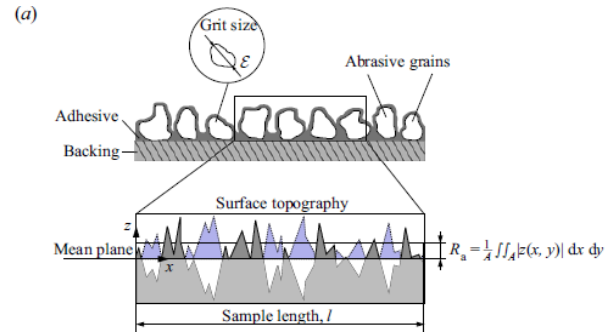
J. Fluid Mech. (2021), vol. 917, A50, doi:10.1017/jfm.2021.313



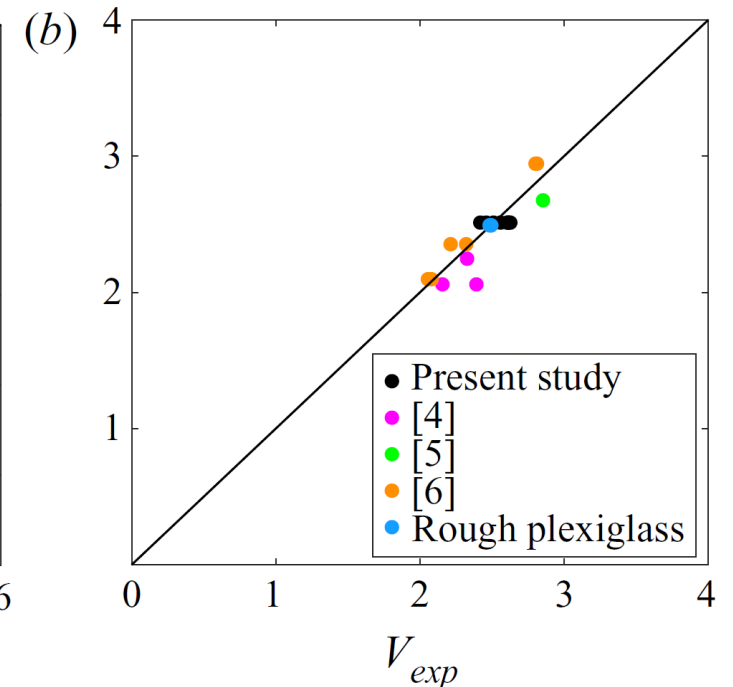
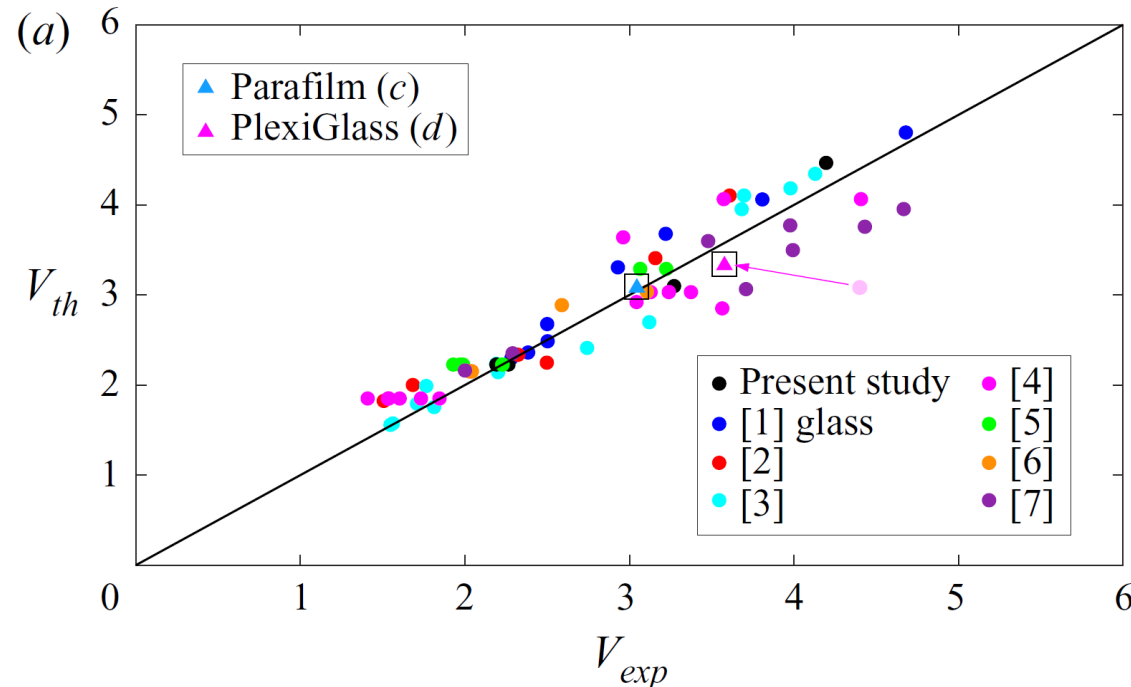
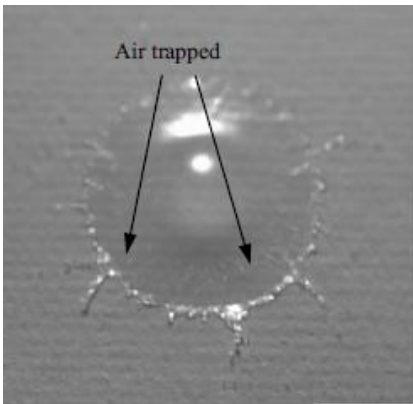
Spreading and splashing of drops impacting rough substrates

P. García-Geijo¹, E. S. Quintero¹, G. Riboux¹ and J. M. Gordillo^{1,†}

¹Área de Mecánica de Fluidos, Departamento de Ingeniería Aeroespacial y Mecánica de Fluidos, Universidad de Sevilla, Avenida de los Descubrimientos s/n, 41092 Sevilla, Spain



$$\alpha = 62.5^\circ - 9^\circ [\theta_{adv}/90^\circ],$$



OUR DESCRIPTION RATIONALIZES THE EXPERIMENTS REPORTED IN PRL AND ALSO THE INFLUENCE OF THE SURROUNDING ATMOSPHERE: SPREADING-SPLASHING-SPREADING TRANSITION

CONDITION FOR SPLASH TRANSITION ONCE THE LIFT FORCE IS CALCULATED INTEGRATING THE PRESSURE DISTRIBUTION AT THE LAMELLA

$$\frac{K_l \mu_g V_t}{\sigma} = K \quad \text{with } K = 2\beta^2 - 0.3\rho_g V_t^2 H_t / \sigma \simeq 0.034,$$

WHICH DEPENDS ON THE RATIO BETWEEN THE SLIP LENGTH AND THE THICKNESS OF THE LAMELLA

if $We \lambda / R < (\mu_g / \mu)^{3/4} Oh^{1/4}$,

$$K_l \simeq \frac{1}{2} \left(\frac{6}{\tan^2 \alpha} \right) \ln \left[0.011 \left(\frac{\mu}{\mu_g} \right)^{3/4} Oh^{-1/4} \left(\frac{H_t}{\lambda} \right) \right]$$

$$We \lambda / R > (\mu_g / \mu)^{3/4} Oh^{1/4} \quad K_l \simeq \left(\frac{6}{\tan^2 \alpha} \right) \ln \left[1 + \frac{H_t}{19\lambda} \right]$$

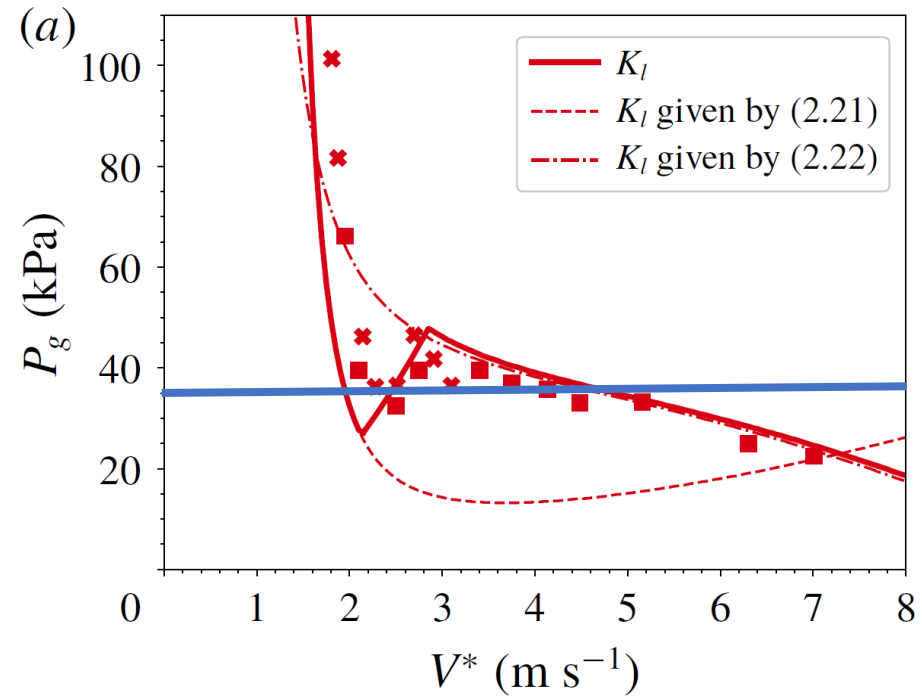
J. Fluid Mech. (2019), vol. 871, R3, doi:10.1017/jfm.2019.396

JFM RAPIDS
journals.cambridge.org/rapids



A note on the aerodynamic splashing of droplets

José Manuel Gordillo^{1,†} and Guillaume Riboux¹



INFLUENCE OF ELECTRIC CHARGE AND SUBSTRATE PERMITTIVITY

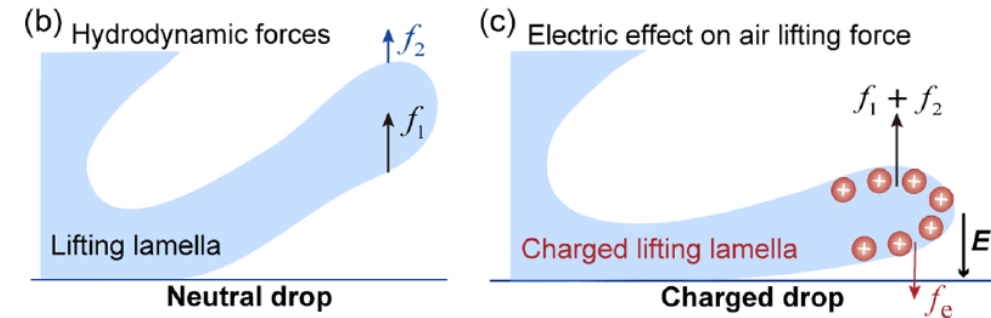
PHYSICAL REVIEW LETTERS **134**, 134001 (2025)

Editors' Suggestion

Featured in Physics

Why Charged Drops Do Not Splash

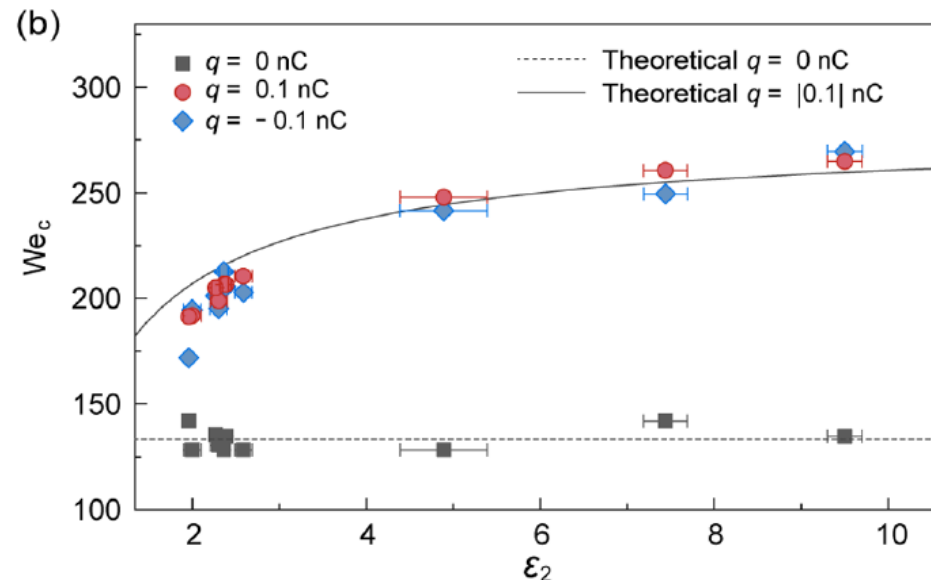
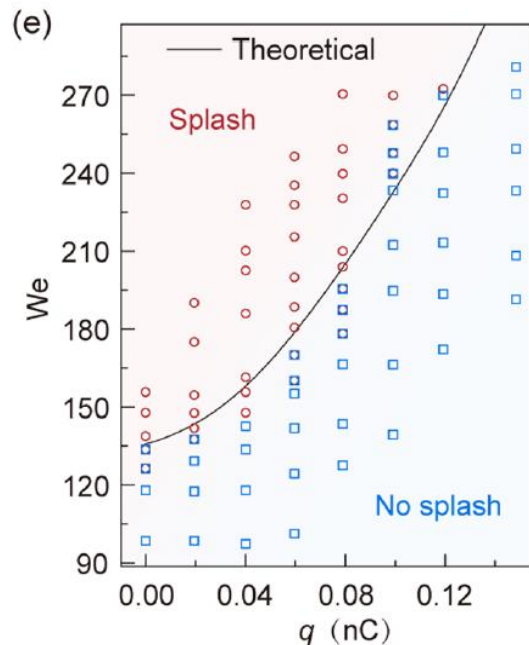
Fanfei Yu^{1,*}, Aaron D. Ratschow^{2,3,*}, Ran Tao⁴, Xiaomei Li⁵, Yuankai Jin¹, Jinpei Wang¹, and Zuankai Wang^{1,†}



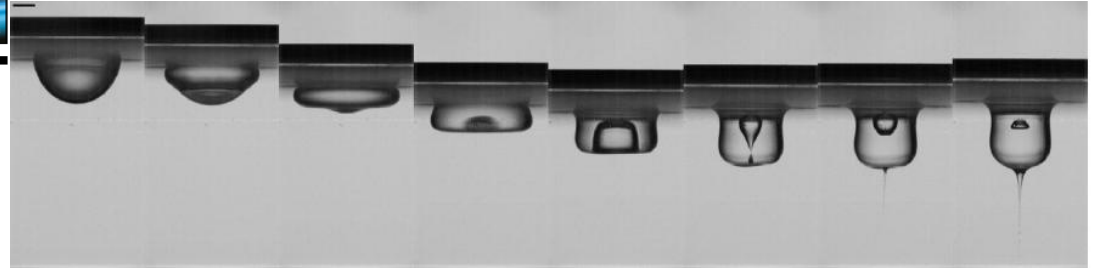
USING OUR RESULTS ONCE THE EFFECT OF THE ELECTRIC FORCE, WHICH POINTS IN THE OPPOSITE DIRECTION TO THAT OF LIFT, IS ADDED

$$\frac{\sqrt{3}}{2} \text{Re}^{-1} t_e^{-1/2} + \text{Re}^{-2} \text{Oh}^{-2} = 1.1 t_e^{3/2}$$

$$\beta^{*2} = (K_1 \mu_g V_t + K_2 \rho_g V_t^2 H_t - f_e) / 2\sigma.$$




THE AUTHORS FIND AN EXCELLENT MATCH BETWEEN OBSERVATIONS AND PREDICTIONS ONCE THE ELECTRIC FORCE IS INCLUDED IN OUR SPLASH MODEL



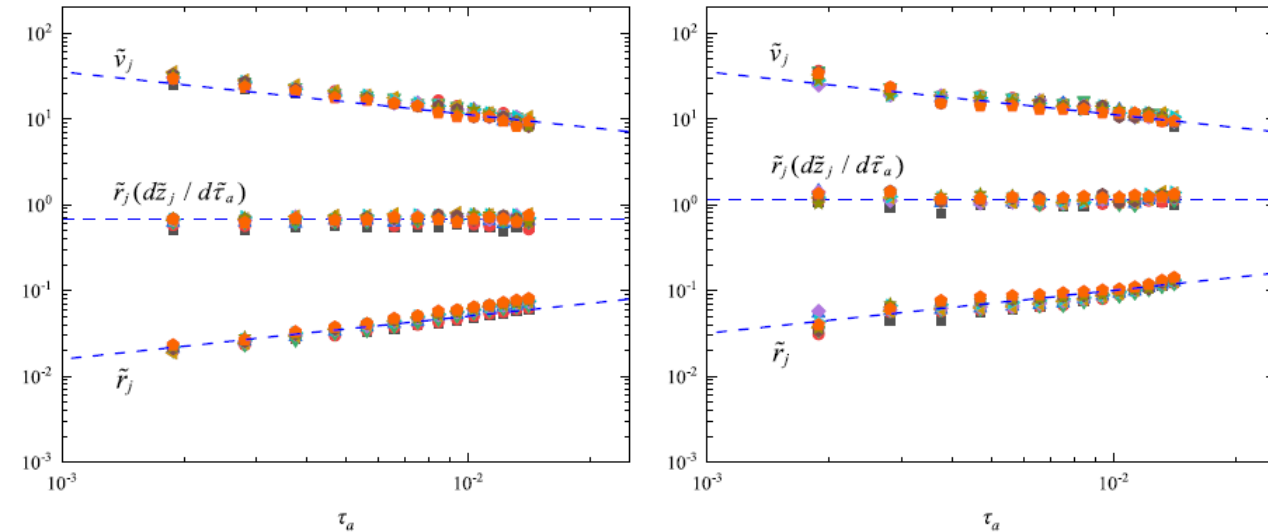
Research Paper

Double bursting jets from a suspended water drop under one cycle of oscillation

Cheng Xu^a, Wanyu Zhu^a, Huihui Xia^b, Weiwei Deng^a ^{*}

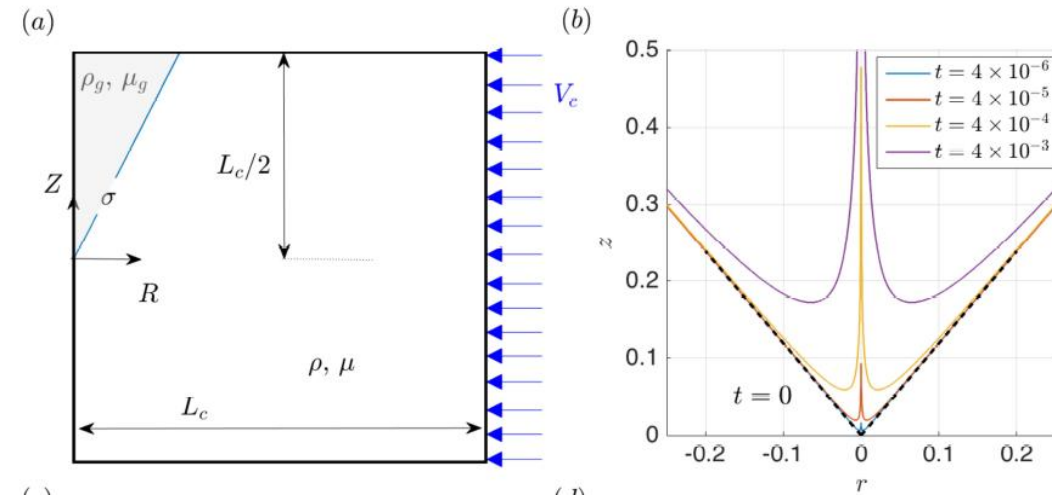
^a Shenzhen Key Laboratory of Soft Mechanics & Smart Manufacturing, Department of Mechanics and Aerospace Engineering, Southern University of Science and Technology, Shenzhen 518055, China

^b Jinxin Technology co., Ltd., Shenzhen 518108, China



cavities of arbitrary shape when their implosion is forced by the radial velocity. Our numerical results confirm the scaling law relationship in the quantitative expression, namely $\tilde{r}_j \propto \tilde{\tau}_a^{1/2}$ and $\tilde{v}_j \propto \tilde{\tau}_a^{-1/2}$, as shown in Fig. 12. The fact that $\tilde{r}_j \tilde{v}_j \simeq \text{const}$ for both inner and outer jets supports the key assumption made by Gordillo and Blanco-Rodríguez (2023) that the dimensionless liquid flow rate per unit length directed towards the axis of symmetry, q_∞ , remains constant in time. The double

CONSTANT FLOW RATE AT THE COLLAPSE STAGE IMPLIES SELF-SIMILARITY, BUT NOT OF INERTIO-CAPILLARY TYPE

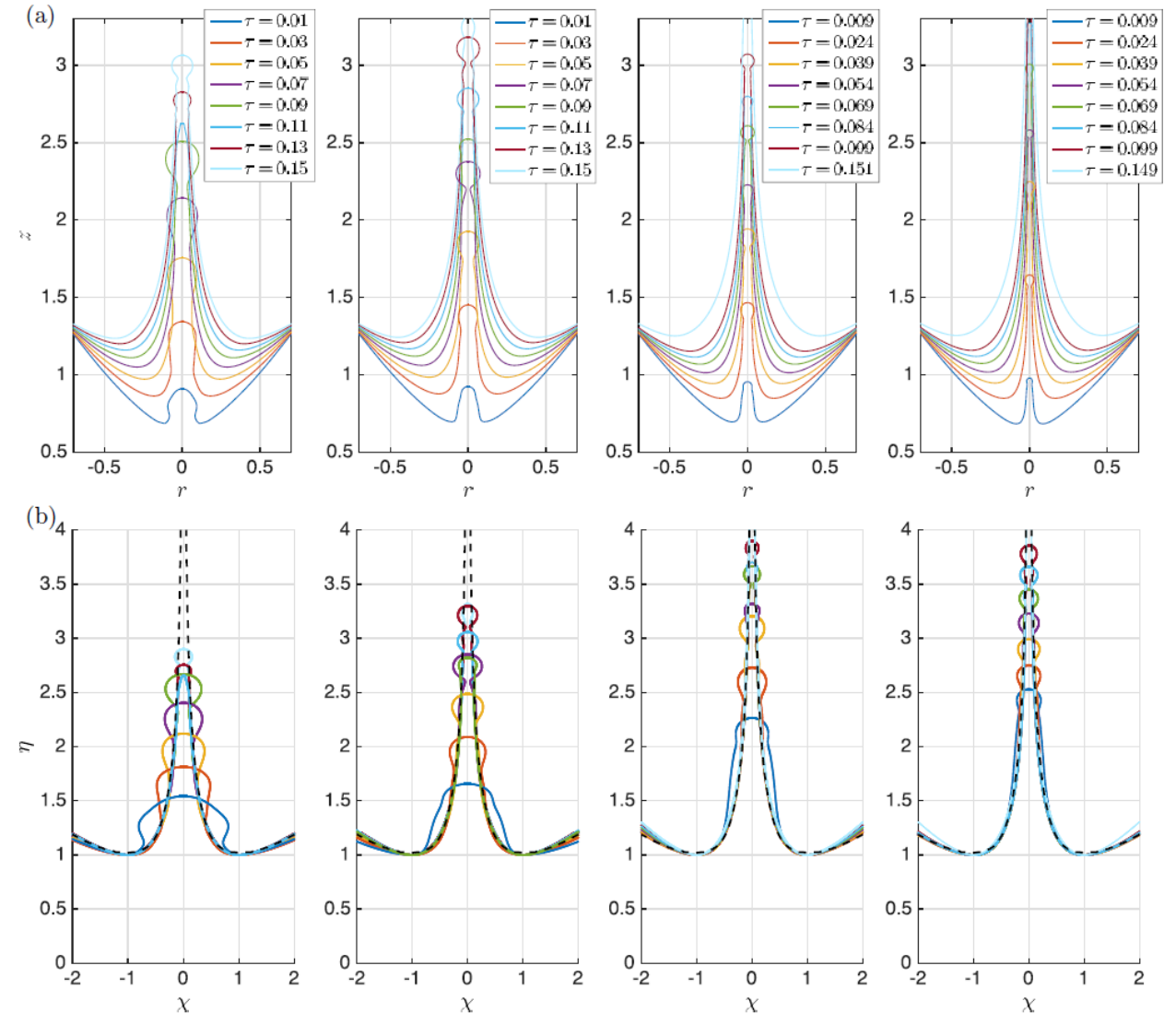


$$Q_\infty \quad \text{and} \quad r = r_s(\tau = 0, z)$$

FOR THE CASE OF CONICAL CAVITIES

$$z_{jet} \propto \sqrt{q_\infty \tau} / \tan \beta$$

$$r_{jet}(\tau) \propto \tan \beta \sqrt{q_\infty \tau}$$



Self-similar recoil of inviscid drops

Asimina Sierou and John R. Lister

Department of Applied Mathematics and Theoretical Physics, University of Cambridge, Wilberforce Road, Cambridge CB3 0WA, United Kingdom

(Received 22 July 2003; accepted 3 February 2004; published online 5 April 2004)

After capillary pinchoff of a fluid thread or drop, the newly created drop tips recoil due to the large local curvature. Similarity solutions for the postpinchoff recoil of an axisymmetric inviscid fluid of density ρ_1 and surface tension γ immersed in a surrounding fluid of density ρ_2 are obtained over a range of the density ratio $D = \rho_2 / \rho_1$. The far-field shape of the two new drops and the far-field dipole potentials are prescribed from known prepinching solutions [D. Leppinen and J. R. Lister, *Phys. Fluids* **15**, 568 (2003)] and the positions and self-similar shape of the two recoiling tips are calculated. The momentum of the prepinching flow makes a significant difference to the recoiling shapes. Capillary waves are observed, in agreement with previous two-dimensional studies and analytical calculations, and the wave frequency is found to increase with D . The recoil of a single axisymmetric drop (with a conical far-field shape) under surface tension is also studied as a function of D and the far-field cone angle θ_0 . Capillary waves are again observed, and the results for small values of θ_0 are shown to agree well with previous asymptotic predictions. The related problem of violent jet emission, following the formation of a near-conical structure with very high curvature at its tip, is also discussed and its similarity with the recoiling cone problem investigated. © 2004 American Institute of Physics. [DOI: 10.1063/1.1689031]

**ANY OF THE INFINITE FAMILY OF SELF-SIMILAR SOLUTIONS
PREDICT THE EXISTENCE OF A LONG JET... AS IT COULD HAVE BEEN
ANTICIPATED FROM THE EXPERIMENTAL EVIDENCE...**

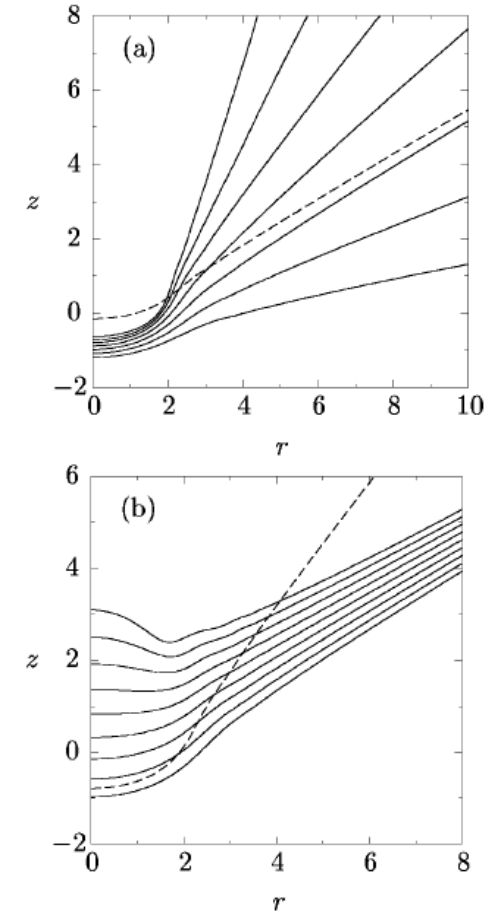
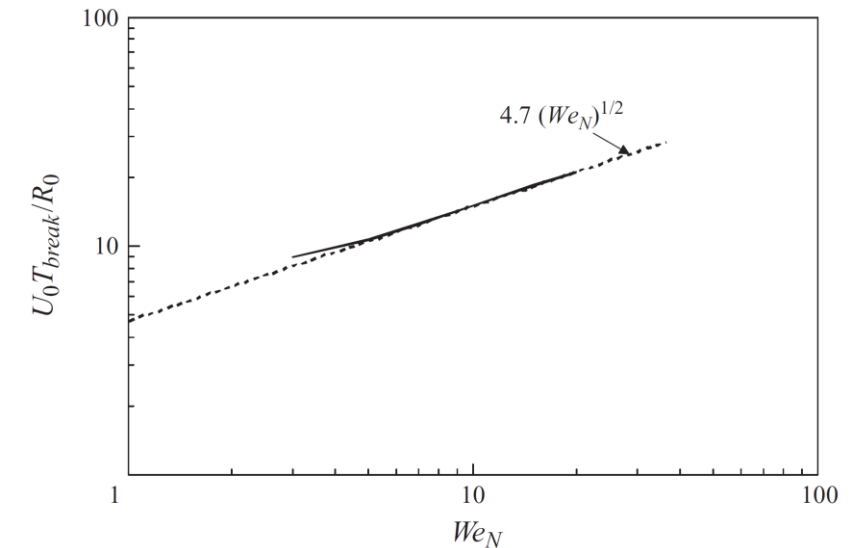
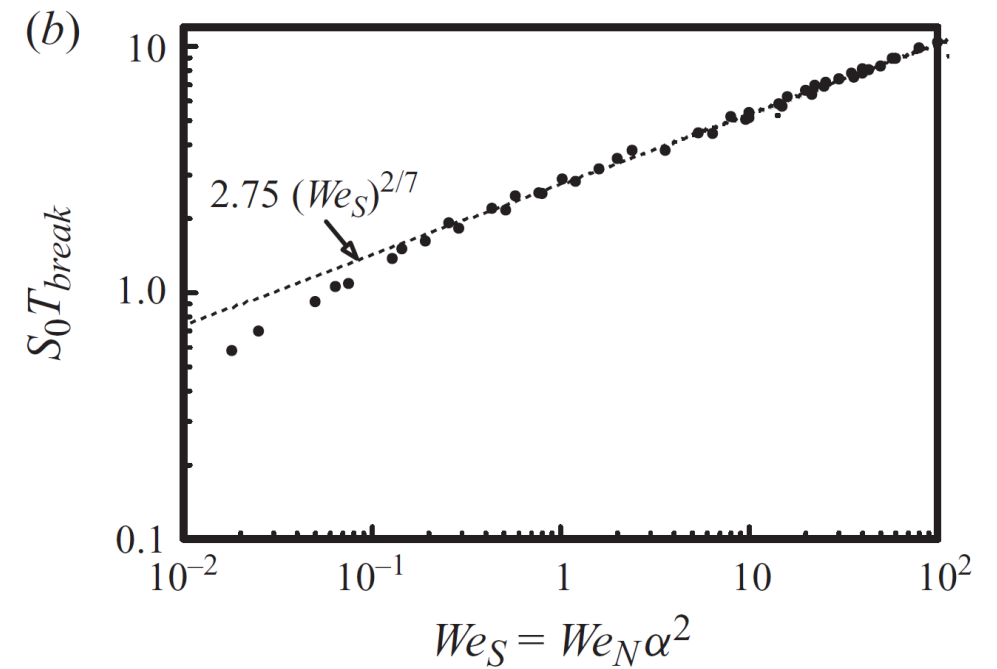
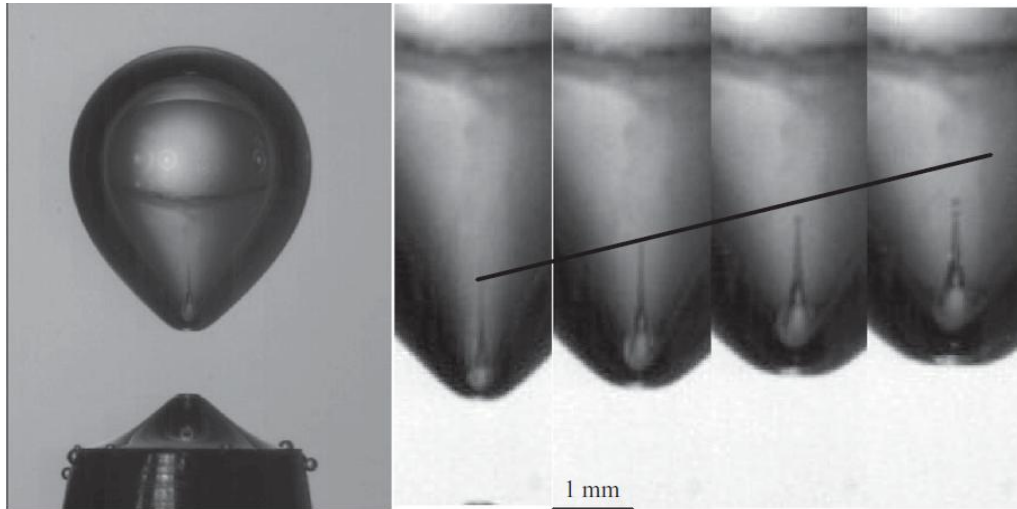


FIG. 16. Two parameter family of self-similar solutions for the collapsing cavity formulation: (a) fixed far-field flow, varying far-field cone angle ($20^\circ \leq \theta_H \leq 80^\circ$) and (b) fixed far-field cone angle ($\theta_H = 60^\circ$), varying far-field flow. The dashed lines are shown for comparison and correspond to a solution which does not belong to each plotted family.

Generation and breakup of Worthington jets after cavity collapse. Part 2. Tip breakup of stretched jets

J. M. GORDILLO^{1†} AND STEPHAN GEKLE^{2,3}

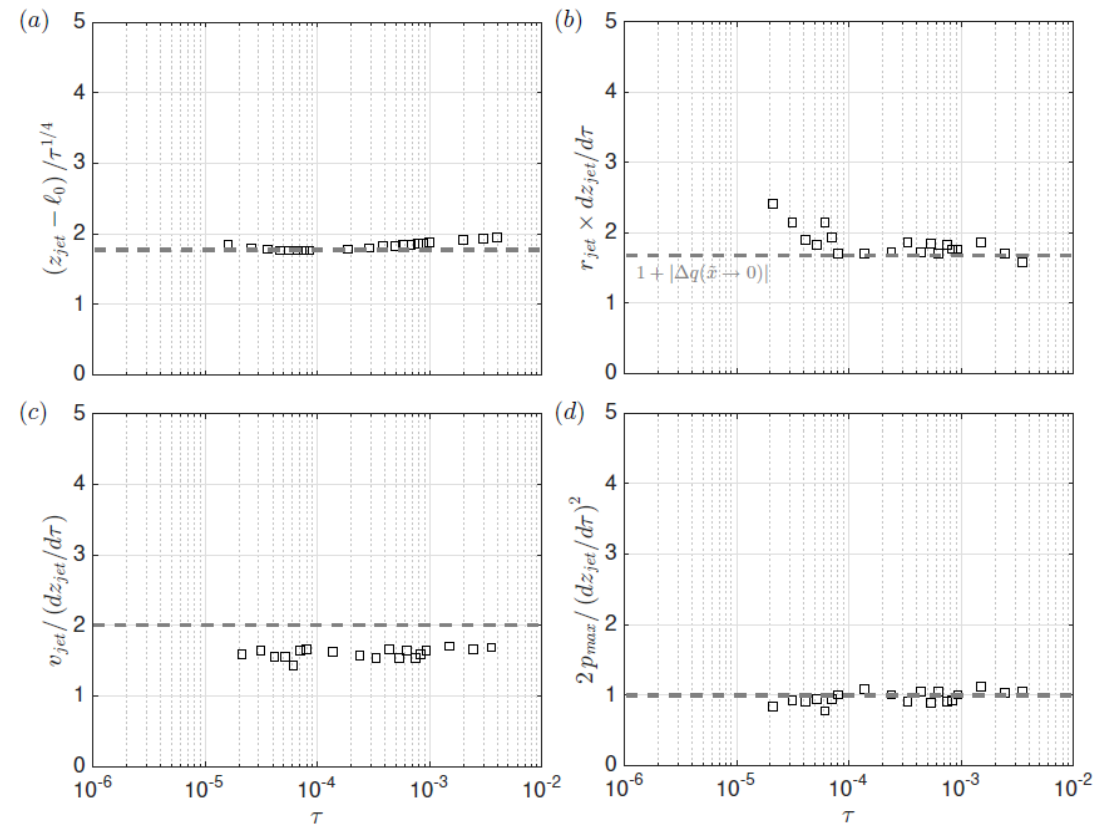
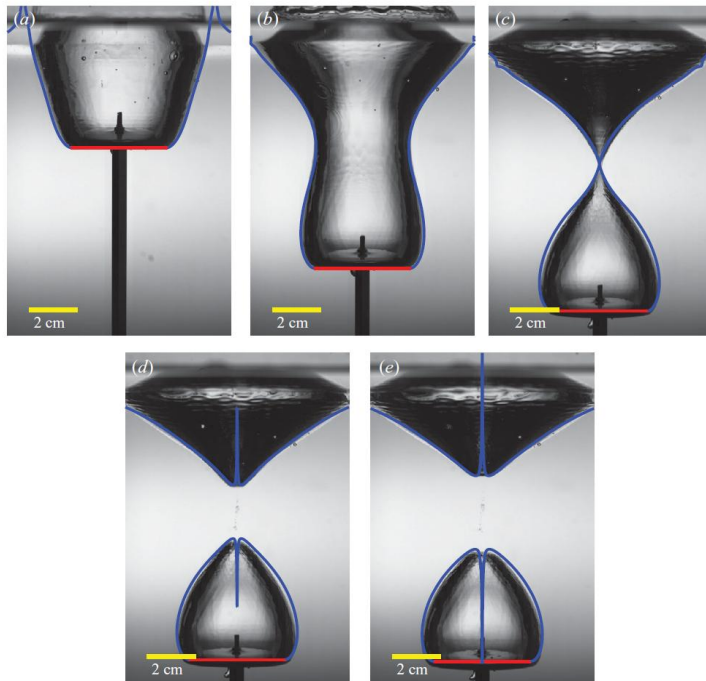


The breakup length is smaller than $\sim 5 R We^{1/2}$

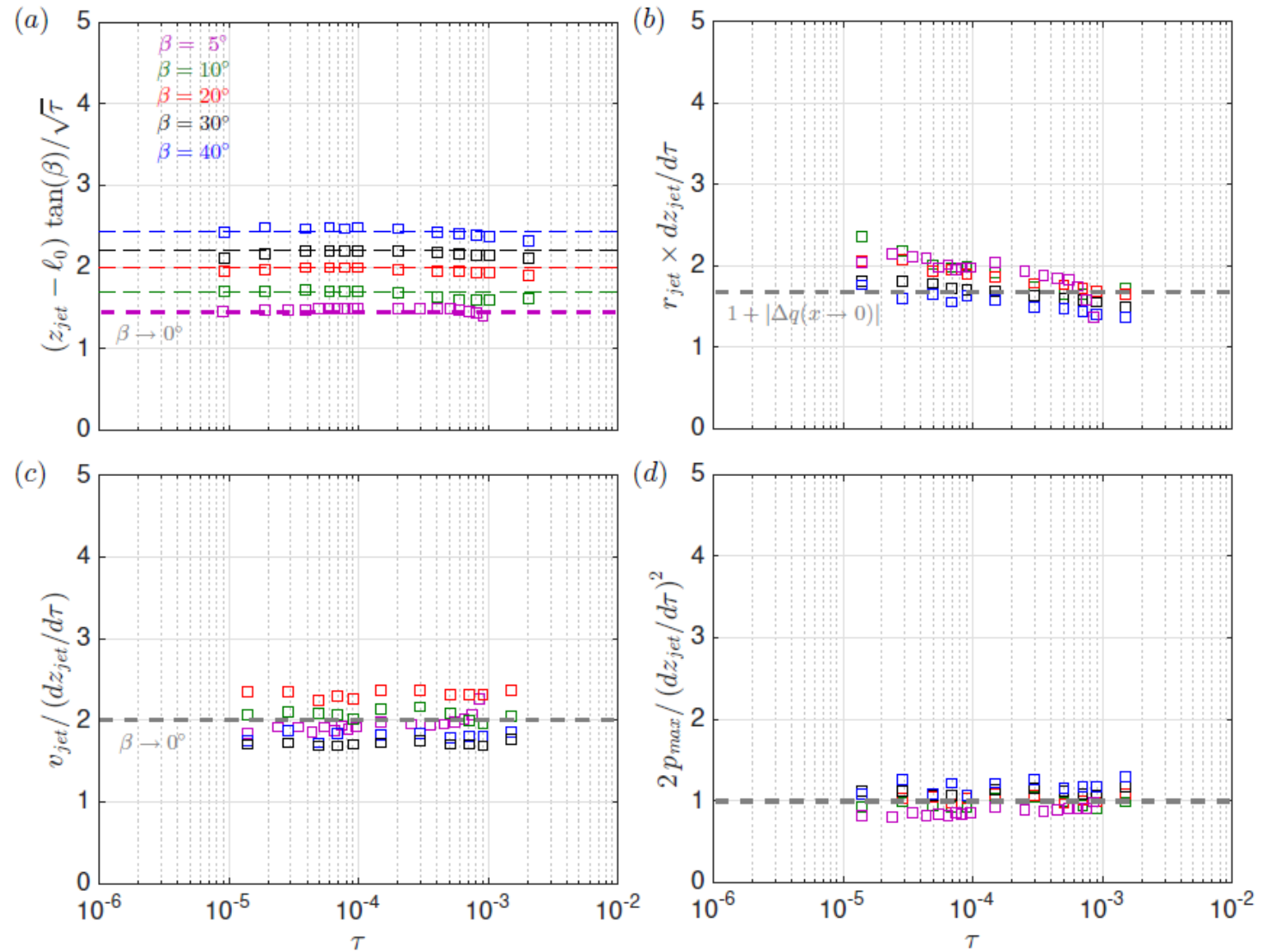
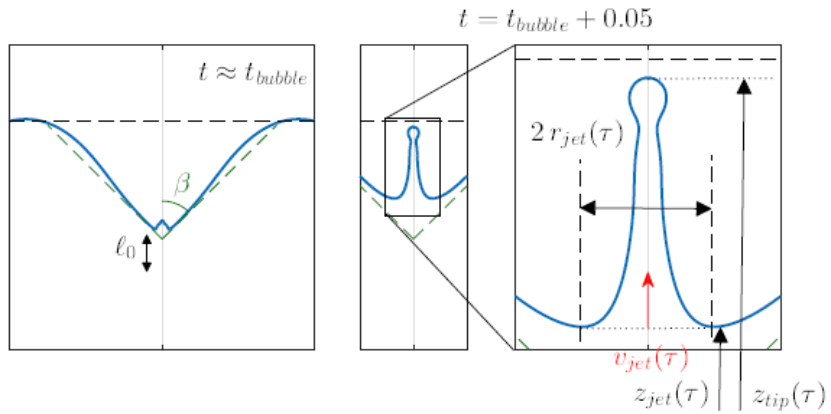
Hence, experimental evidence already indicates that $We \gg 1$ and,

Hence, also that the inertio-Capillary balance is inconsistent with experimental observations

COMPARISON BETWEEN NUMERICAL SIMULATIONS AND PREDICTIONS, PARABOLIC CAVITIES, INCOMPRESSIBLE SIMULATIONS

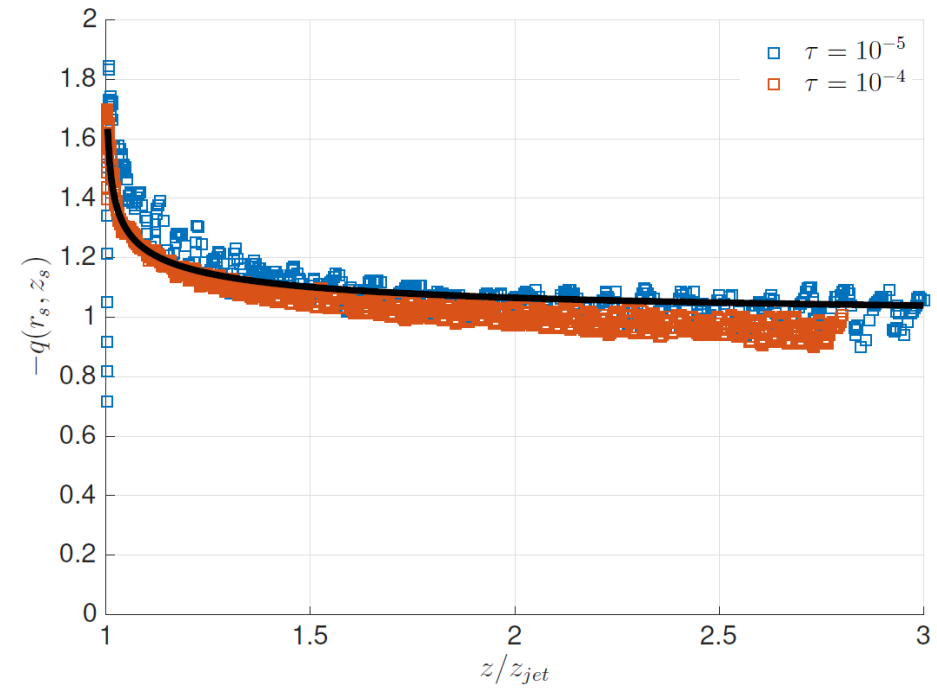
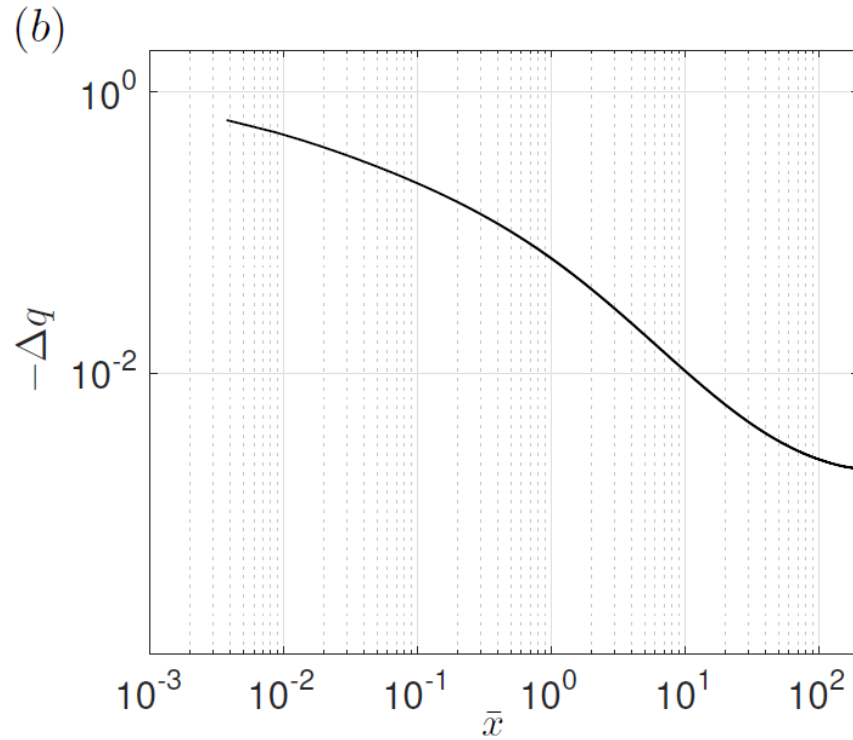


COMPARISON BETWEEN NUMERICAL SIMULATIONS AND PREDICTIONS CONICAL CAVITIES



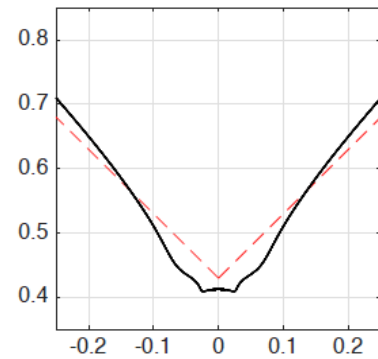
ANALYTICAL DESCRIPTION OF $\mathbf{r_{jet}(\tau)}$, $\mathbf{z_{jet}(\tau)}$ AND $\mathbf{u_{jet}(\tau)}$ FOR THE CASE OF SLENDER CAVITIES-I

$$\bar{z} = \frac{z}{z_{jet}(\tau)}, \quad \bar{z}_0 = \frac{z_0}{z_{jet}(\tau)}, \quad \Delta q = \frac{df}{d\bar{z}} \quad \int_1^\infty \frac{df}{d\bar{z}} d\bar{z} = f_\infty = -1 \quad \frac{1}{\bar{z}-1} - \frac{1}{\bar{z}+1} + \int_1^\infty \frac{df/d\bar{z}_0 (\bar{z} - \bar{z}_0) d\bar{z}_0}{\left[(\bar{z} - \bar{z}_0)^2\right]^{3/2}} = 0.$$



$$Oh = \mu / \sqrt{\rho R_b \sigma}, \quad La = Oh^{-2},$$

$La = 2500$



$La \geq 2500,$

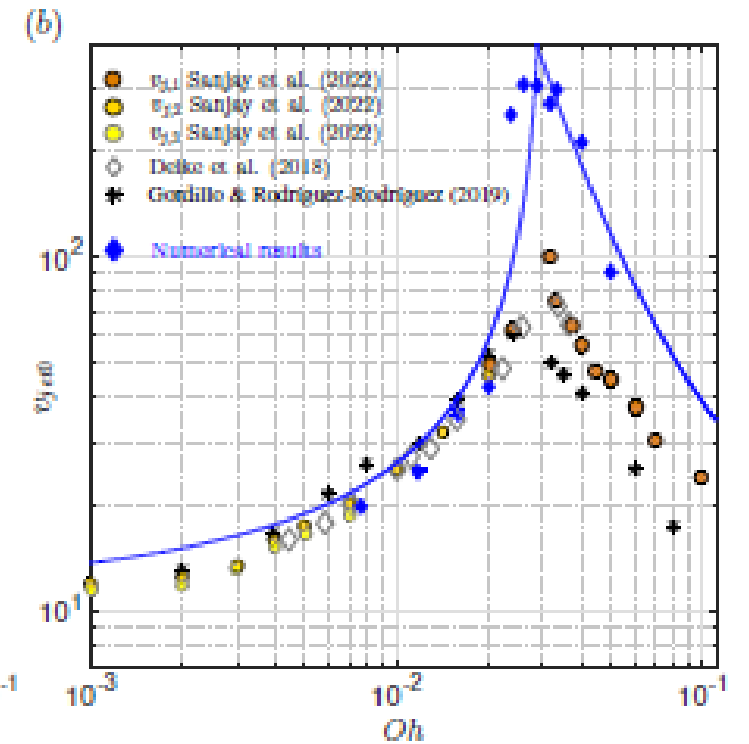
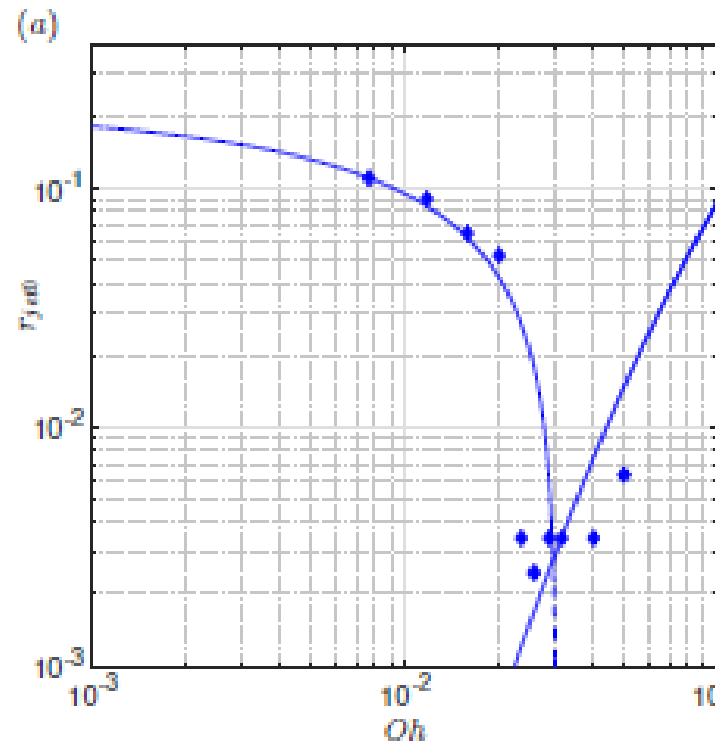
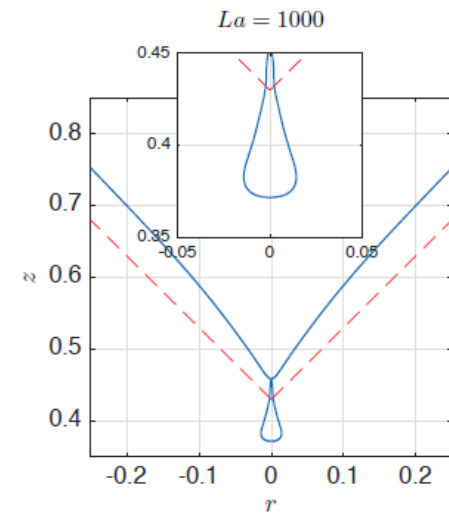
$$r_{jet0}(La) = 0.2215 \left(1 - \sqrt{\frac{Oh}{0.0305}} \right),$$

$$v_{jet0}(La \geq 2500) \simeq 2.5 / r_{jet0}(La).$$

$La < 2500$

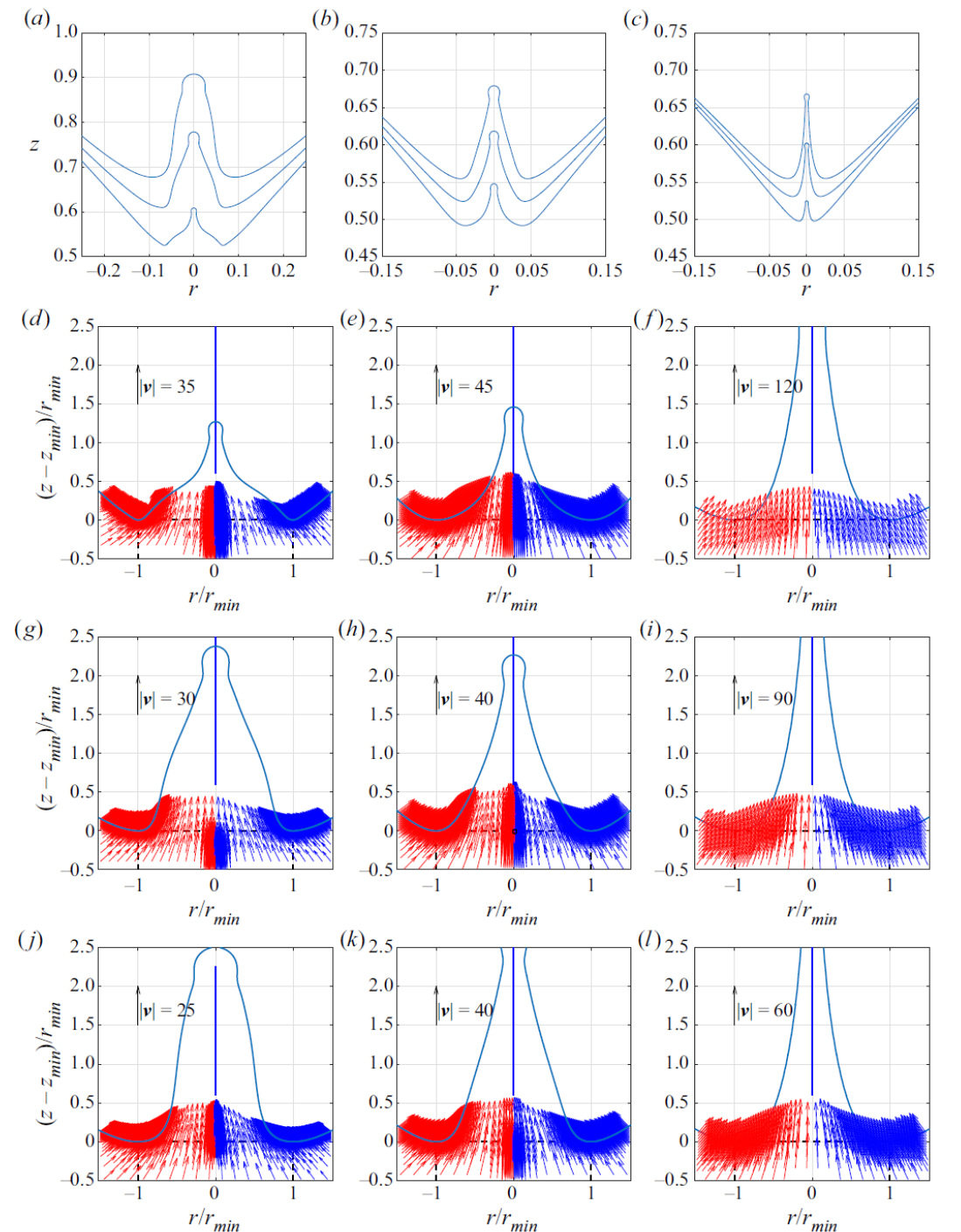
$$r_{jet0}(La < 2500) = r_0(0) \times \exp \left(-\frac{1}{2} \left[\left[\ln \left(\frac{-KOh r_0(0)}{(2r_c r_0 \dot{r}_0)(0)} \right) \right]^2 - \left[\ln \left(\frac{r_0(0)}{2r_c(0)} \right) \right]^2 \right] \right)$$

$$v_{jet0}(La < 2500) = \frac{3.4q_\infty(r_{jet0})}{r_{jet0}} = \frac{3.4KOh}{r_{jet0}(La < 2500)} \quad (6)$$



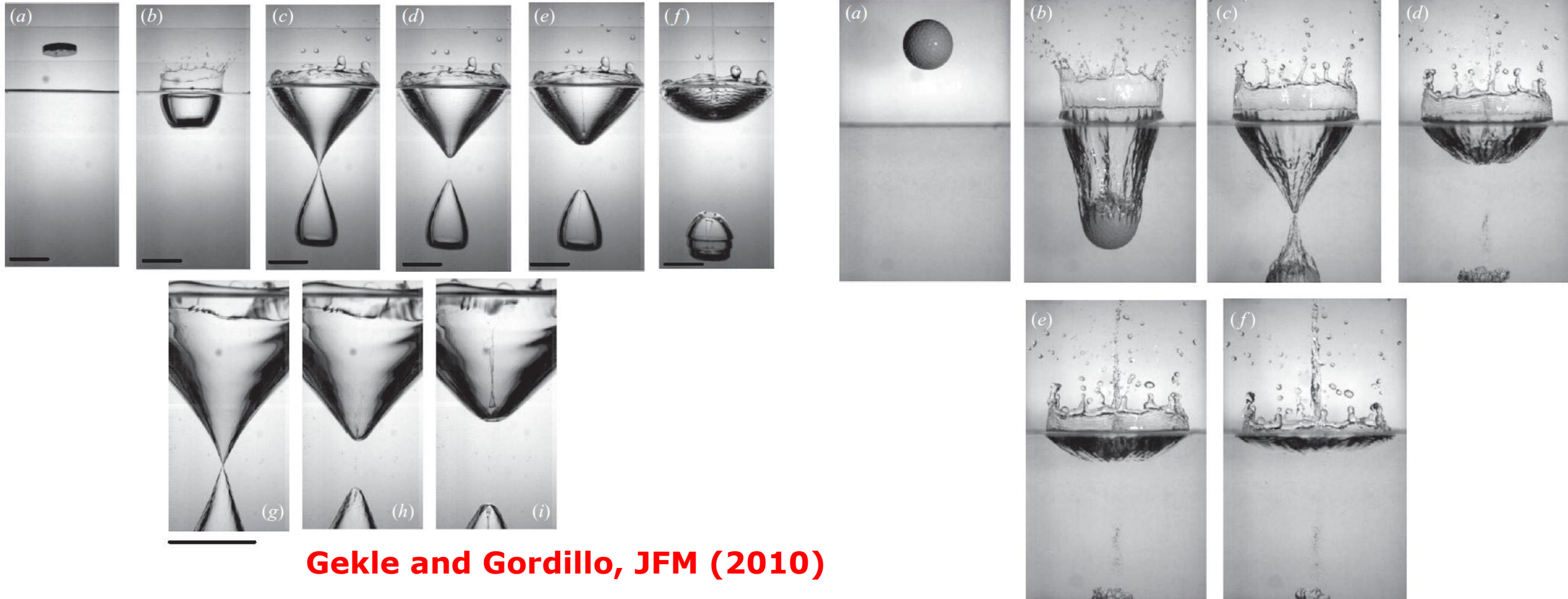
On the jets produced by drops impacting a deep liquid pool and by bursting bubbles

Francisco J. Blanco-Rodríguez¹ and J. M. Gordillo^{1,†}



COMPARISON BETWEEN NUMERICAL SIMULATIONS AND PREDICTIONS, BUBBLE BURSTING JETS-V

Initial values of the jet radius and velocity: asymmetric cutoff radius

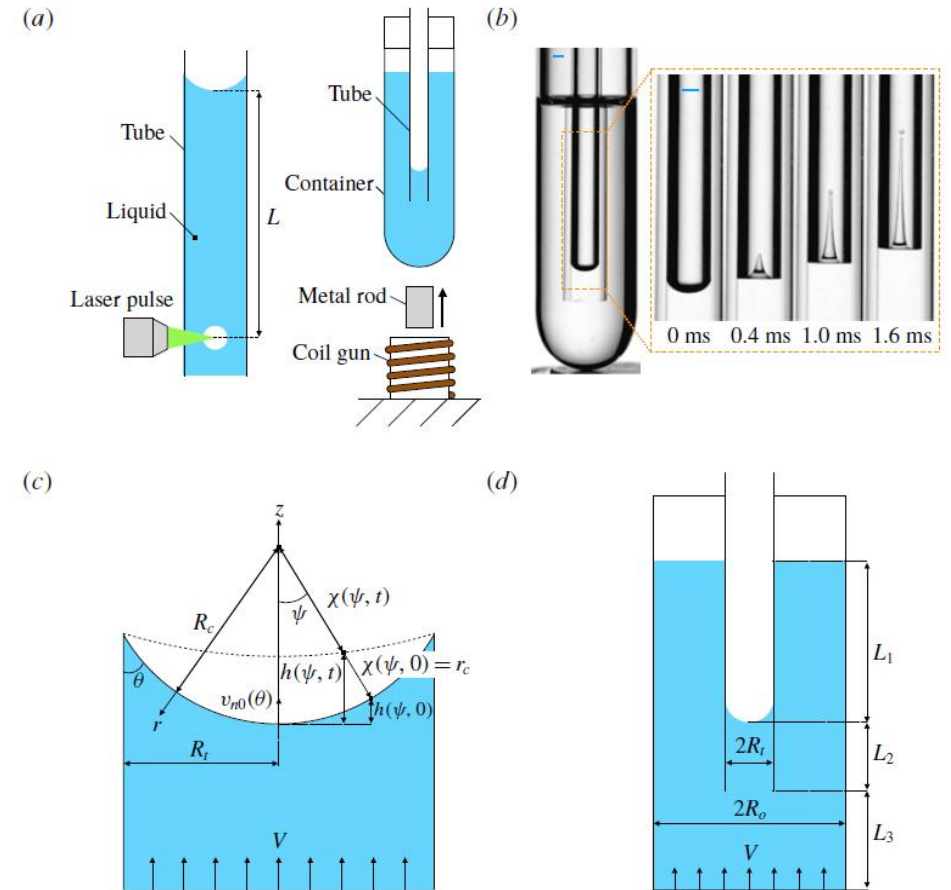


Impulsive generation of jets by flow focusing

José Manuel Gordillo^{1,†}, Hajime Onuki² and Yoshiyuki Tagawa^{2,†}

¹Área de Mecánica de Fluidos, Departamento de Ingeniería Aeroespacial y Mecánica de Fluidos,
Universidad de Sevilla, Avenida de los Descubrimientos s/n 41092, Sevilla, Spain

²Department of Mechanical Systems Engineering, Tokyo University of Agriculture and Technology,
Nakacho 2-24-16, Koganei, Tokyo, Japan



COMPARISON BETWEEN NUMERICAL SIMULATIONS AND PREDICTIONS, UNIFORM FLOW RATE-I

Supersonic needle-jet generation with single cavitation bubbles

Cite as: Appl. Phys. Lett. **118**, 134103 (2021); doi: [10.1063/5.0045705](https://doi.org/10.1063/5.0045705)

Submitted: 28 January 2021 · Accepted: 15 March 2021 ·

Published Online: 1 April 2021 · Publisher error corrected: 19 April 2021



View Online

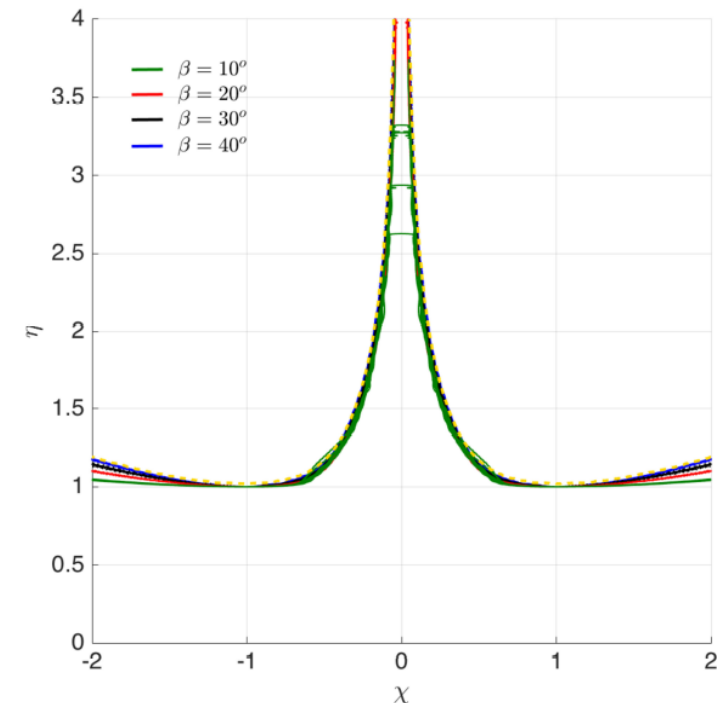
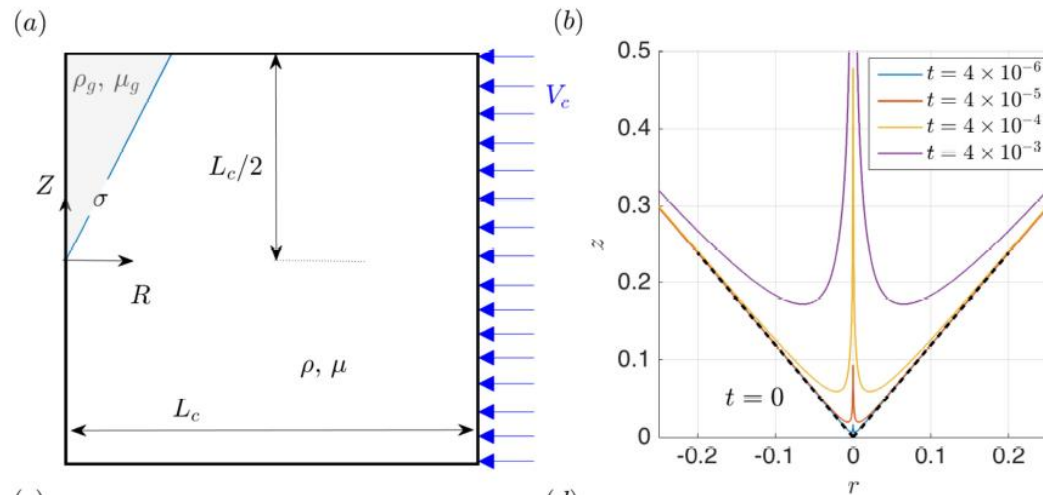


Export Citation



CrossMark

Fabian Reuter^{a)} and Claus-Dieter Ohl

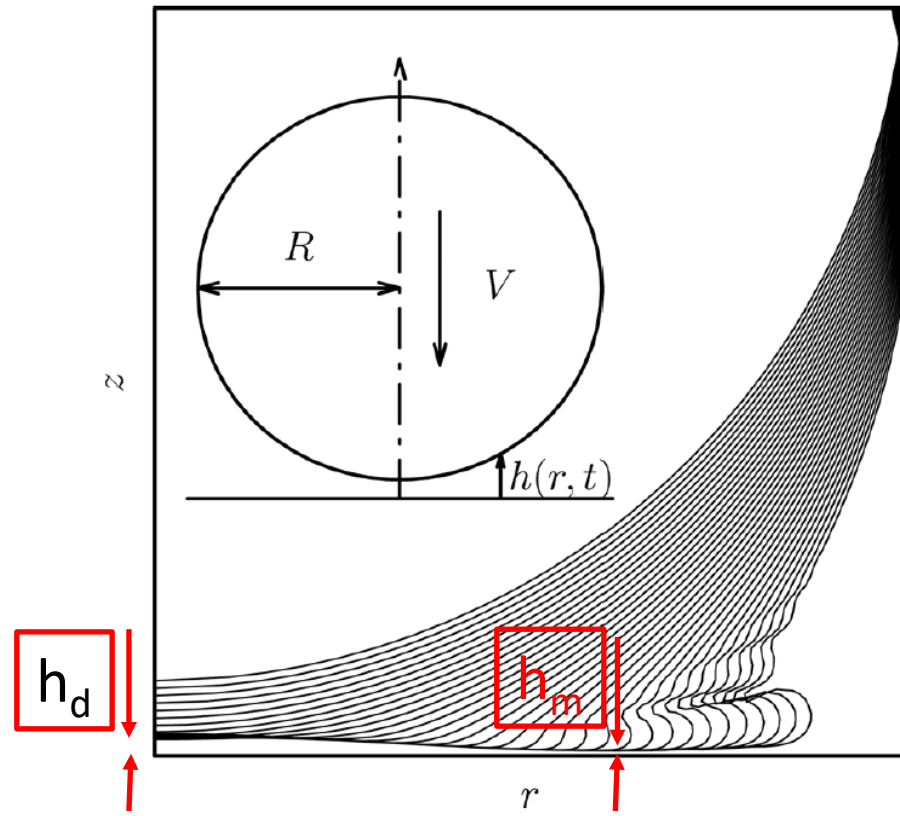


We find a new self-similar solution for the case of the implosion of conical cavities

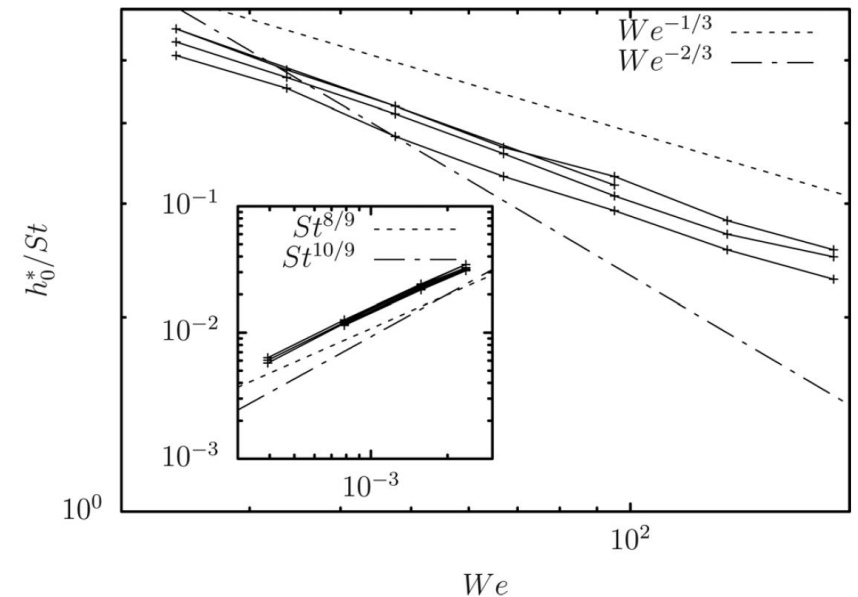
Curvature singularity and film-skating during drop impact

Laurent Duchemin¹ and Christophe Josserand²

$$St = \frac{\rho UR}{\mu_a}, \quad We = \frac{\rho U^2 R}{\sigma}$$



$$h_d \simeq 2.8RSt^{-2/3}.$$



Numerical simulations show that the minimum thickness at the periphery of the entrapped bubble coincides with our prediction

$$\frac{h_{m,c}}{R} \propto We^{-1/3} St^{-10/9}.$$

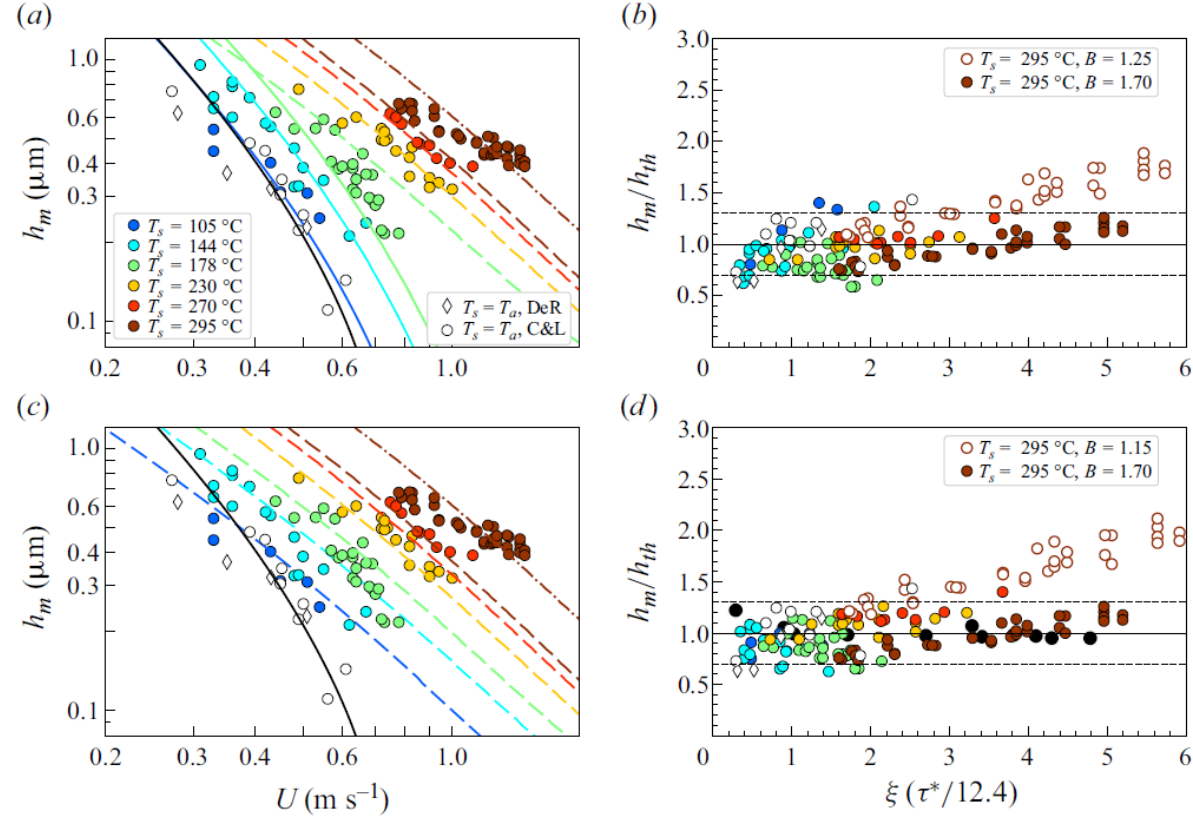
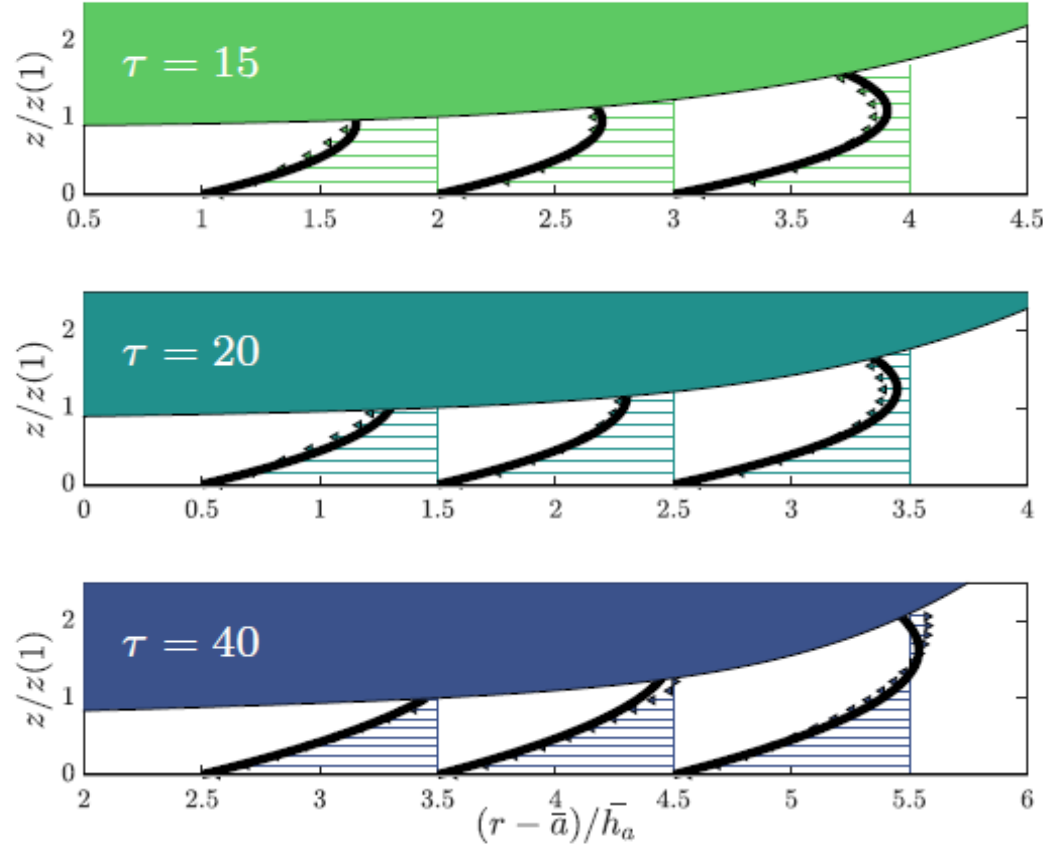


Figure 8. (a) Comparison between the predictions given in (4.14)–(4.16) and the values for the minimum thickness of the air or vapour layers measured by de Ruiter *et al.* (2012) (DeR) and Chantelot & Lohse (2023) (C&L) for different values of the impact velocity U and for different values of the substrate temperature T_s . Here, the values of the effective gas viscosity and the effective gas conductivity have been modified taking into account kinetic effects through (4.7)–(4.12). Solid lines represent the predictions for h_m corresponding to the capillary regime, whereas the predictions for h_m in the inertial regime are represented using dashed lines. (b) Comparison between the predicted and measured values of h_m in (a) as a function of ξ . (c) The experimental data are compared here only with the predictions given by (4.16). In this case, the value of the prefactor is 1.15 instead of 1.25. (d) Comparison between the predicted and measured values of h_m in (c) as a function of ξ . The dashed horizontal lines in (b,d) are placed at 1 ± 0.3 .



Normalized radial velocity field u/\dot{a} beneath the impacting drop represented in the moving frame of reference, e.g. the wetted radius velocity $\dot{a} = \sqrt{3}/2 s^{-1/2}$, at three different normalized radial positions $r - \bar{a}/\bar{h}_a$ for the case $We = 22$ and $St = 2.12 \times 10^4$.

$$-\frac{h_m^3}{12\mu_a} \frac{\partial p}{\partial r} - \frac{V_m h_m}{2} \approx 0,$$

Capillary regime,

$$h_m = 3.5R\tau^{2/3}We^{-1/3}St^{-10/9}$$

$$-\frac{\partial p}{\partial r} \propto \frac{\rho U^2}{R} \tau^{-11/6} St^{14/9} We^{2/3}$$

$$u_{th} = \frac{1}{2}U \left(-\frac{\partial p}{\partial r} \frac{R}{\rho U^2} \right) \left(\frac{St}{R^2} \right) \left[z(z-h) \right] + \frac{\sqrt{3}}{2}U\tau^{-1/2} \left[K(\tau) \frac{z}{h} - 1 \right]$$